

**SYSTEMATIC REVIEW**

# Evaluating Knee Osteoarthritis Induction Methods in Small Translational Animal Models from 1970-2025: A Comprehensive Systematic Review

Armin Arabzadeh, MD; Shervin Mossavarali, MD; Gita Manzari Tavakoli, MD; Kasra Mirzaei, MD; Ayda Manzari Tavakoli, MD; Brian T. Feeley, MD; Mohammad Hossein Nabian, MD

*Research performed at Center for Orthopedic Trans-Disciplinary Applied Research, Tehran University of Medical Sciences, Tehran, Iran*

Received: 15 August 2025

Accepted: 26 November 2025

**Abstract**

**Objectives:** This approaches, for inducing knee osteoarthritis (KOA) in rabbit and rodent models. It also summarizes data study evaluates surgical, mechanical, chemical, genetic, and diet-induced methods, as well as combination-based on post-intervention time points for KOA development, the duration required for osteophyte formation, KOA scoring systems, and relevant histopathological findings.

**Methods:** A systematic search of PubMed, Scopus, and Web of Science (from 1970 to February 2025) was conducted using the PICO framework, focusing on animal models (rabbits and rodents), osteoarthritis induction methods, comparative efficacy, and relevant outcomes. Extracted variables included model characteristics, interventions, and KOA-related findings. The risk of bias was assessed using the Cochrane risk-of-bias tool and the ROBINS-I tool.

**Results:** After screening 5,702 records, 98 studies met the inclusion criteria. Surgical (n = 34), chemical (n = 15), genetic (n = 13), mechanical (n = 19), and high-fat diet-induced (n = 6) models, as well as combination approaches, were reviewed. Among surgical techniques, anterior cruciate ligament transection (ACLT) and medial meniscus destabilization (DMM) were the most frequently used, whereas monosodium iodoacetate (MIA) was the predominant chemical inducer. Genetic models primarily involved gene deletions or mutations in C57BL/6 mice. Mechanical induction methods included joint loading, treadmill running, and immobilization. Histological evaluation—most commonly using the Mankin and Osteoarthritis Research Society International (OARSI) scoring systems—was the predominant approach for KOA assessment, while micro-computed tomography (micro-CT) was employed in selected studies. Osteophyte formation was prominent in surgical and specific chemical models and was typically observed within 8 weeks post-intervention. Additionally, each induction method exhibited a distinct time course for osteophyte development and the establishment of KOA.

**Conclusion:** Each approach offers distinct advantages for replicating KOA pathology and for facilitating research into disease mechanisms and therapeutic interventions.

**Level of evidence:** N/A (since this study reviews the laboratory/basic science studies)

**Keywords:** Animal model, Induction method, knee, Osteoarthritis, Rabbit, Rodents

**Introduction**

**K**nee osteoarthritis (KOA) is the most common inflammatory and progressive degenerative disorder of articular cartilage in orthopedics, accounting for approximately 85% of osteoarthritis cases worldwide.<sup>1</sup> The global prevalence of KOA is estimated at 16.0% among individuals aged 15 years and older, with an

incidence rate of 203 per 10,000 person-years in those aged 20 years and older.<sup>2</sup> The incidence of KOA increases with age, and the number of cases is projected to rise by 74.9% between 2020 and 2050.<sup>3</sup> Given the aging global population and the strong association between advanced age and the increasing incidence of KOA,<sup>2</sup> It is crucial to

**Corresponding Author:** Mohammad Hossein Nabian, Center for Orthopedic Trans-Disciplinary Applied Research, Tehran University of Medical Sciences, Tehran, Iran

**Email:** dr.nabian.cotar@gmail.com



THE ONLINE VERSION OF THIS ARTICLE  
ABJS.MUMS.AC.IR



further elucidate the pathophysiology of this disease and the risk factors that contribute to its development. Animal models play a critical role in KOA research by facilitating the development of targeted therapies and enabling the evaluation of novel pharmacological treatments and surgical interventions, ultimately contributing to improved patient care strategies.<sup>4</sup>

Numerous studies using animal models have established reproducible approaches for inducing KOA.<sup>5-8</sup> Small animal models, including rabbits and rodents, are widely employed because of their rapid disease progression, ease of handling, and relatively low cost, making them well-suited for investigating the pathogenesis and pathophysiology of KOA.<sup>5</sup> These models exhibit histological alterations and patterns of disease progression that closely resemble those observed in human KOA.<sup>5</sup> Moreover, entire knee joints from rabbits and rodents can be sectioned histologically, allowing comprehensive evaluation of gross morphological, radiological, ultrastructural, and histopathological changes.<sup>9</sup>

The most common techniques for inducing KOA include surgical, chemical, and mechanical methods. Among surgical approaches, anterior cruciate ligament transection (ACLT), medial and lateral collateral ligament transection (MCLT and LCLT), and destabilization of the medial meniscus are the most frequently employed.<sup>10-13</sup> Common mechanical approaches for KOA induction include joint compression with peak loading or obesity applied to the medial femoral condyles, knee immobilization in extension using a plastic splint, long-distance running, and obligatory bipedal locomotion.<sup>14-17</sup> Chemical methods primarily involve intra-articular injections of monosodium iodoacetate (MIA), hydrogen peroxide (H<sub>2</sub>O<sub>2</sub>), bacterial collagenase, interleukin-17 (IL-17), and papain.<sup>10,18-21</sup> In addition, genetic induction models involving RNA alterations, as well as high-fat diet regimens, have also been employed to induce KOA.<sup>22,23</sup>

Few studies have provided a comprehensive analysis of data concerning post-intervention time points for KOA development, KOA scoring systems, and associated histopathological findings.<sup>24,25</sup> This systematic review aims to address these gaps by examining rabbit and rodent models across a range of induction techniques, including surgical, mechanical, chemical, genetic, diet-induced, and combination approaches. A graphical abstract summarizing the main findings of this study is presented in [Figure 1].

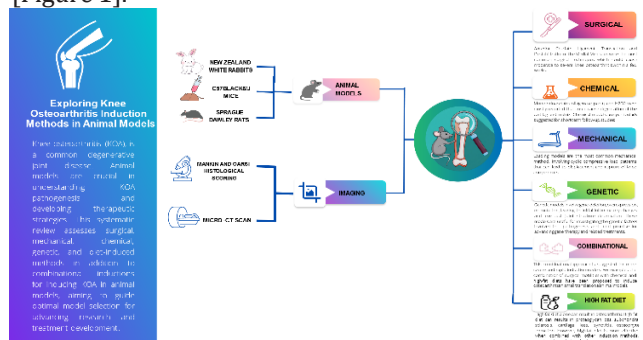


Figure 1. Knee Osteoarthritis Induction Methods in Small Translational Animal Models

## Materials and Methods

The protocol for the current systematic review is consistent with the Preferred Reporting Items for Systematic Reviews and Meta-Analyses (PRISMA) statements.<sup>26</sup> This study was registered within the International Prospective Register of Systematic Reviews (PROSPERO ID: CRD420251155300)

### 1. Search Strategy

A systematic search of Web of Science, PubMed, and Scopus was conducted to identify studies published between 1970 and February 2025, without restrictions on publication type. Medical Subject Headings (MeSH) and Emtree terms were incorporated to maximize the retrieval of relevant records. The search strategy included the following keywords and their corresponding synonyms and equivalents: rodent, rabbit, jird, gerbil, vole, capybara, Hydrochoerus, jerboa, Dipodidae, beaver (Castor), chinchilla, guinea pig (Cavia), hamster, Cricetidae, Oryctolagus cuniculus, Oryctolagus, hare, bunny, cottontail, lapin, cony, leveret, Lepus, lagomorph, mouse, mice, house mouse, Mus domesticus, Mus musculus, rat, laboratory rat, Norway rat, Wistar rat, Sprague-Dawley rat, Murinae, New Zealand rabbit, knee, osteoarthritis, osteoarthrosis, arthrosis, gonitis, gonarthrosis, gonarthrosis, joint degeneration, cartilage damage, bone spurs, animal model, animal experimentation, animal research, animal experimental use, animal experiment, induced model, experimental model, spontaneous model, genetically modified model, negative model, and orphan model. The detailed search syntax for each database is provided in [Supplementary Material 1]. In addition, the reference lists of all included studies were manually screened to identify potentially eligible articles not retrieved through the database search. All stages of the systematic search were performed collaboratively by AA, GMT, SM, and KM.\*

### 2. Study Selection and Eligibility Criteria

The PICO framework guided study selection: the population comprised animal models; the intervention involved inducing knee osteoarthritis; the comparison evaluated the efficacy and limitations of different induction methods; and the outcomes focused on osteoarthritis-related measures.

Studies were included if they investigated methods for inducing knee osteoarthritis (KOA) in rabbit or rodent models and were published in English. Eligible induction methods comprised mechanical, chemical, surgical, genetic, high-fat diet-induced, or combination approaches. No restrictions were applied regarding publication date or country of origin. Exclusion criteria included studies evaluating therapeutic interventions or pharmacological effects, spontaneously developed KOA models, osteoarthritis affecting joints other than the knee, human studies, different forms of arthritis, studies conducted in non-rodent or non-rabbit models, review articles, book chapters, technical notes, letters to the editor, and publications in languages other than English.

### 3. Data Collection and Extraction

After duplicate records were removed using EndNote, four authors (AA, GMT, SM, and KM) independently screened the titles and abstracts of all retrieved studies. The full texts of potentially eligible articles were subsequently assessed for inclusion by the same authors. Any disagreements or conflicts arising during the screening process were resolved through discussion with MHN and BTF.

Data extraction was performed independently by AA, GMT, SM, and KM, with MHN and BTF consulted to resolve any disagreements. Extracted data encompassed study characteristics (number of models, species, sex, age, and weight), intervention details (type and method of osteoarthritis induction and post-intervention assessment time points), and outcomes. The primary outcomes included osteoarthritis occurrence, KOA scores, and osteophyte formation, including the timing of onset. Secondary outcomes comprised histological, radiographic, and gross morphological findings related to KOA.

For data synthesis and interpretation, outcomes were categorized by induction method. Reference management was performed using EndNote, while data extraction, handling, and coding were conducted using Microsoft Excel.

### 4. Risk of Bias Assessment

The methodological quality and risk of bias of each included study were independently assessed by two reviewers (AMT and GMT) using the Cochrane Risk of Bias tool (RoB 2.0), the most recent version available.<sup>27</sup> The following domains were evaluated: bias arising from the randomization process, bias due to deviations from intended interventions, bias due to missing outcome data, bias in outcome measurement, and bias in the selection of the reported results. Any discrepancies or disagreements between the reviewers were resolved through discussion with MHN and BTF until consensus was reached. Visual summaries of the risk-of-bias assessments were generated using ROBVIS (Risk-of-Bias Visualization Tool).<sup>28</sup>

## Results

### • Study Selection

A total of 5,702 records were identified through database searches. After duplicate removal, 5,074 records were screened, of which 4,835 were excluded based on title and abstract screening. Subsequently, 239 full-text articles were assessed for eligibility. Of these, 152 were excluded, primarily because they were irrelevant to the study question, insufficiently reported eligibility criteria, were review articles, were non-English publications, were book chapters, or were unavailable reports. An additional 11 records were identified through manual searching. Ultimately, 98 studies were included in this systematic review. The PRISMA flow diagram

illustrating the study selection process is presented in [Figure2].

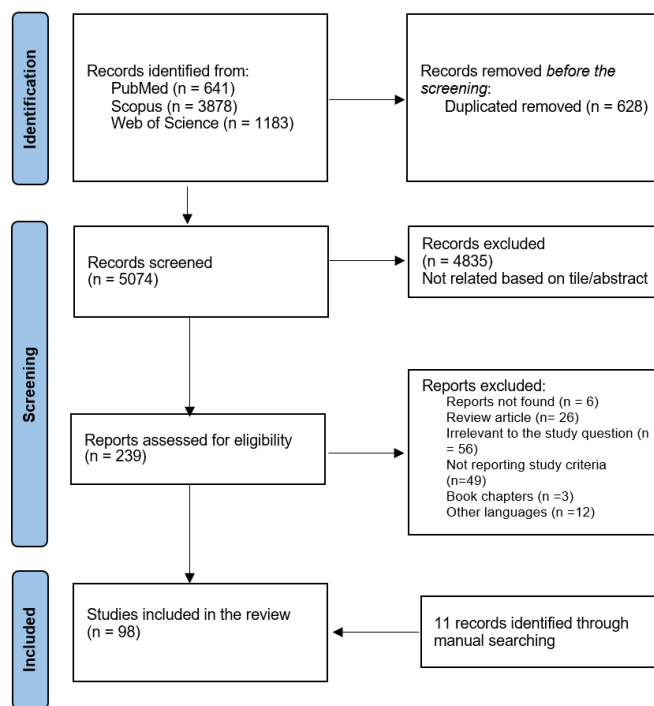


Figure 2. PRISMA chart

### • Characteristics of the Included Studies

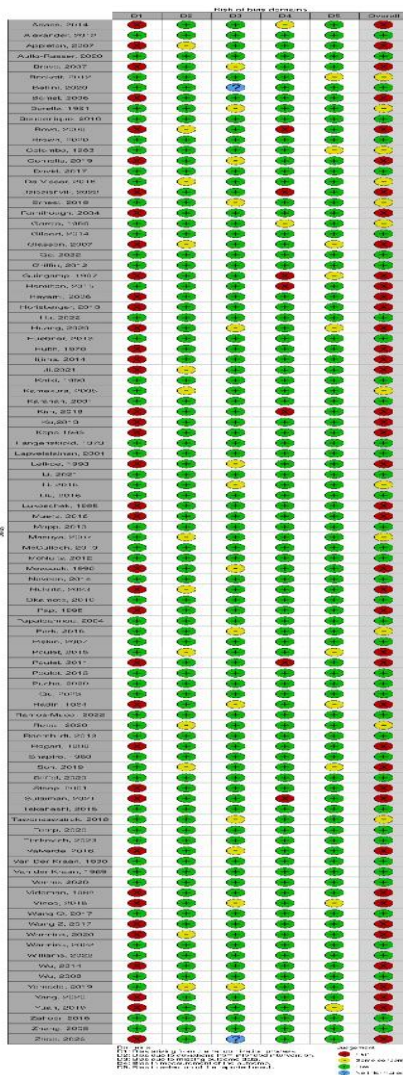
Among the 98 included studies, 34 reported surgical induction of KOA, encompassing 1,036 animals aged 8 weeks to adulthood.<sup>11-13,29-59</sup> Fifteen studies investigated chemical induction methods, including 563 animals aged between 8 weeks and 1 year.<sup>18,19,21,60-71</sup> Thirteen studies employed genetic induction models involving 204 animals, aged from birth to 10 weeks.<sup>22,23,72-83</sup> Nineteen studies used mechanical induction methods in 754 animals aged 8 weeks to 2 years.<sup>14,84-101</sup> Six studies examined high-fat diet-induced KOA, involving 178 animals aged 8-12 weeks.<sup>17,102-106</sup> Ten studies reported data on both surgical and chemical induction methods,<sup>10,20,107-114</sup> while one study included both mechanical and surgical induction.<sup>115</sup> Additionally, four studies reported the use of combination induction methods.<sup>10,18,37,71</sup>

### • Risk of Bias Assessment of the Included Studies

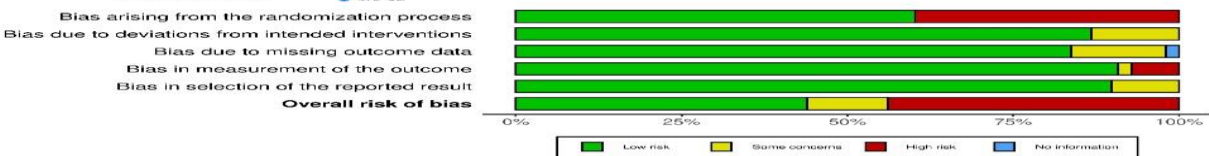
Among the 98 included studies, 43 were judged to have a low risk of bias, 12 raised some concerns, and 43 were assessed as

having a high risk of bias. Overall, most studies were methodologically robust with respect to randomization (D1), deviations from intended interventions (D2), missing outcome data (D3), and outcome measurement (D4), with the majority rated as low risk across these domains. Only a small number of studies raised concerns due to incomplete reporting of the randomization process or insufficient detail in the measurement of outcomes. The most frequent source of bias

was identified in the selection of reported results (D5), where many studies were rated as high risk because of selective or incomplete reporting and a lack of clarity regarding prespecified analysis plans. Despite these concerns, no studies were excluded for high risk of bias; however, findings from studies with concerns in D5 were interpreted with appropriate caution. A detailed overview of the risk-of-bias assessments for the included studies is presented in [Figures 3A and 3B].



A



B

Figure 3A,B.ROBVIS: Risk-of-bias VISualization. (A) Traffic Light Plot for risk of bias domains, including D1: Bias arising from the randomization process, D2: Bias due to deviations from intended intervention, D3: Bias due to missing outcome data, D4: Bias in measurement of the outcome, D5: Bias in selection of the reported result. (B) Overall bar plots of the distribution of risk-of-bias for each domain.

- **Types of Intervention**

All data about the surgical, chemical, mechanical, genetic, high-fat diet, and combination induction groups are presented in [Supplementary Tables 1–6], respectively.

- **Surgical Inductions**

The most commonly reported surgical interventions include destabilization of the anterior cruciate ligament (ACL), posterior cruciate ligament (PCL), medial collateral ligament (MCL), lateral collateral ligament (LCL), and both the medial and lateral menisci. Among the various surgical methods used to induce KOA, anterior cruciate ligament transection (ACLT)<sup>10,11,13,30-32,41,42,48,50,54,56,57,107,108,114</sup> and destabilization of the medial meniscus (DMM)<sup>13,34,35,44-46,52,113</sup> were the most frequently employed, likely due to their effectiveness and relative ease of implementation. In addition, some studies induced KOA through direct cartilage injury,<sup>32,40,47,51,52</sup> one study utilized ovariectomy (OVX),<sup>31</sup> and another reported the placement of a plastic device within the knee joint.<sup>53</sup> Detailed information on all surgical procedures, including post-intervention time points, the duration required for osteophyte formation, and KOA scores, is provided in [Supplementary Table 1].

- **Chemical Induction**

Chemically induced KOA models involve intra-articular injection of chemical agents to disrupt joint homeostasis and cause structural damage.<sup>10</sup> Across the included studies, seven different substances were used: monosodium iodoacetate (MIA),<sup>10,31,60,62-64,66-69,107-109,112,113</sup> collagenase,<sup>19,65,69,70,114</sup> papain,<sup>21,69,71</sup> hydrogen peroxide (H<sub>2</sub>O<sub>2</sub>),<sup>18</sup> stromal cell-derived factor 1 (SDF-1),<sup>111</sup> interleukin-17 (IL-17),<sup>20</sup> and interleukin-1 (IL-1).<sup>70</sup> Considerable heterogeneity was observed in the concentrations administered as well as in the animal species used, and some chemical induction protocols did not result in successful KOA development. Among these agents, MIA was by far the most frequently used, administered at a wide range of doses across different animal models. Detailed information on each chemical agent, including concentration, animal model, post-intervention assessment time points, time to osteophyte formation, and KOA scores, is summarized in [Supplementary Table 2].

- **Mechanical Induction**

Mechanical induction methods were classified into three major categories: loading,<sup>14,84,86-91,93,94,96-98,100,101,115</sup> running,<sup>92,95</sup> and immobilization.<sup>85,99</sup> Among these, loading-based models were the most frequently applied and exhibited substantial variability in parameters such as duration, rate, force magnitude, and other secondary

factors. Data on running and immobilization models were limited, as only two studies used each technique. Detailed information on the specific mechanical interventions, including post-intervention assessment time points, the duration required for osteophyte formation, and KOA scores, is provided in [Supplementary Table 3].

- **Genetic Induction**

Genetic induction models were categorized by mouse strain, with C57BL/6 mice most commonly used for KOA induction.<sup>23,80,81</sup> The majority of these models involved either targeted gene deletions or mutations.<sup>23,80</sup> Notably, deletion of genes such as ephrin-B2, MIG-6, and Alj5 was associated with the most rapid osteophytic changes.<sup>72,79,82</sup> Detailed information on genetic induction models, including post-intervention assessment time points, the duration required for osteophyte formation, and KOA scores, is presented in [Supplementary Table 4].

- **Combinational Inductions and A High-Fat Diet**

A high-fat diet is frequently used in combination with other induction methods, most commonly surgical approaches,<sup>102-105</sup> although a high-fat diet alone has also been shown to induce KOA.<sup>104,106</sup> When used as a sole induction method, KOA development typically requires a longer time course, as summarized in Supplementary Table 5. In addition, several other combination induction strategies have been reported,<sup>10,18,37,71</sup> which are detailed in Supplementary Table 6. High-fat diet-based models and their combination approaches were intentionally presented in separate tables and were therefore not included in the corresponding single-method tables.

- **Animal Species**

After excluding 14 genetic studies due to differences in animal models, the remaining 85 studies collectively used 13 distinct animal species. The most frequently used species were New Zealand White rabbits,<sup>10,11,20,29-31,39,40,43,47,49,50,53,58,60-62,70,71,87,97,107,115</sup> C57BL/6J mice,<sup>17,33-35,41,44,46,52,84,88-90,93,104,106</sup> Sprague–Dawley rats,<sup>14,31,37,48,51,55,56,98,105,108,109,112-114</sup> and Wistar rats,<sup>18,32,42,45,54,63-68,92,94,95,101,102,105,110</sup> which were used in 23, 15, 14, and 18 studies, respectively. Three studies did not specify the exact rabbit strain used,<sup>59,85,99</sup> and were therefore categorized as a separate group. Within surgical induction models, New Zealand White rabbits, C57BL/6J mice, and Sprague–Dawley rats were the most commonly used species for KOA induction. Specifically, 18 studies utilized New Zealand White rabbits,<sup>10,11,20,29-31,39,40,43,47,49,50,53,58,107</sup> 15 studies employed C57BL/6J mice,<sup>33-35,41,44,46,52</sup> and 15 studies used Sprague–Dawley rats.<sup>31,37,48,51,55,56,108,109,112-114</sup> Detailed information is provided in [Supplementary Table 1]. For chemical

induction models, New Zealand White rabbits<sup>10,20,60-62,70,71,107</sup> and Wistar rats<sup>18,63-68,110</sup> were the two most frequently used species, appearing in 23 and 21 studies, respectively [Supplementary Table 2]. In contrast, genetic induction models involved a wider diversity of species, and in some cases, hybrid or modified strains were generated; nevertheless, C57BL/6J mice<sup>23,77-83</sup> were the predominant species used for genetic manipulation [Supplementary Table 3]. Among mechanical induction models, a total of 39 experimental groups employed C57BL/6J mice<sup>84,88-90,93</sup> and rabbits,<sup>85,99</sup> with each species used in 10 studies, making them the most commonly utilized animals in this category (Supplementary Table 4). The specific animal species used in each induction group are detailed in [Supplementary Tables 1–6].

#### • *Diagnostic Procedure to Investigate the Establishment of KOA*

In all 98 included studies, histological evaluation of knee cartilage was performed to determine the presence and severity of KOA. Several studies applied standardized scoring systems to assess and compare KOA severity at different post-intervention time points across experimental groups. Among these, the Mankin score, modified Mankin score, and Osteoarthritis Research Society International (OARSI) score were the most frequently used. Detailed information regarding scoring systems is summarized in Supplementary Tables 1–6. Sixty-six studies relied exclusively on histological assessment,<sup>10-14,17,21,22,29,30,32-35,38-40,42-44,46,48-51,53-58,60-68,70,72,75-77,80,82,87,89,90,92,94,95,97,98,101,103,104,106,108-110,112-115</sup> whereas 32 studies combined imaging modalities with histological assessment.<sup>18-20,23,31,36,37,41,45,47,52,59,69,71,73,74,78,79,81,83-86,88,91,93,96,99,102,105,107,111</sup> Only one study relied exclusively on imaging-based assessment.<sup>100</sup> Among imaging modalities, micro-computed tomography (micro-CT) was the most commonly employed technique. The most relevant KOA-related findings for each induction group are summarized in the final columns of [Supplementary Tables 1–6].

#### *1.1. Osteophyte Formation*

Osteophyte formation was reported in 97 experimental groups.<sup>10,12,17,19,20,23,29,30,34,36-39,41-44,47,49,52,53,55,56,59,60,63,65-67,69,71,74,79,81,82,84-86,90,96,99,102-105,107,109-111</sup> Among the 66 surgical groups, osteophyte formation was observed in 33 groups<sup>10,12,20,29,30,34,36,38,39,41-44,47,49,52,53,55,56,59,109-111</sup>, including five anterior cruciate ligament transection (ACLT) groups (out of 18)<sup>10,30,41,42,56</sup> and 4 destabilization of the medial meniscus (DMM) groups (out of 9)<sup>34,44,52</sup>. In 18 of these 33 surgical groups, osteophytes were detected at 8 weeks or earlier<sup>12,20,30,36,38,39,41,43,44,49,52,53,55,56,109,110</sup>, including 3 ACLT groups<sup>30,41,56</sup> and 4 DMM groups<sup>34,44,52</sup>. The longest time point at which osteophyte formation was observed following surgical induction was 16 weeks.<sup>29,34,59</sup> Among the 67 chemical induction groups, osteophyte

formation was reported in 30 groups,<sup>19,20,60,63,65-67,69,71,107,110,111</sup>, including 13 monosodium iodoacetate (MIA) groups (out of 33 total MIA groups).<sup>60,63,66,67,69,107,110</sup> In 22 of these 30 chemical groups, osteophytes were detected within 4 weeks or less,<sup>19,20,60,63,65-67,69,71,107,110,111</sup>, including 11 MIA groups.<sup>60,63,66,67,69,107,110</sup> The longest reported time point for osteophyte detection among chemical induction models was 12 weeks.<sup>20,111</sup> For mechanical induction models, osteophyte formation was observed in 7 loading groups (84, 90, 96) and six immobilization groups.<sup>85,99</sup> All data related to osteophyte formation are summarized in [Supplementary Tables 1–6].

## Discussion

### *Main Findings*

Our analysis indicated that the most frequently studied animal models included New Zealand White rabbits, Wistar rats, Sprague–Dawley rats, and C57BL/6J mice. Surgical induction methods, such as destabilization of the medial meniscus, were particularly effective at rapidly inducing severe KOA in rodent models. Mechanical models, including joint overload induced by treadmill running or gait alterations, were especially valuable for investigating early-stage KOA and associated biomechanical changes. Compared with other approaches, chemical and surgical induction methods generally led to more rapid progression to moderate to severe osteoarthritis. Chemically induced KOA was characterized by early inflammatory changes but demonstrated a slower overall disease progression, whereas surgically induced KOA showed a delayed onset followed by more severe pathological changes. In contrast, genetic models were frequently associated with alterations in bone structure and involvement of other organs, underscoring the pleiotropic effects of genetic modifications.

### *Comparison of Different Categories*

Within the mechanical category, the primary induction approach involves loading protocols, which may include single or repeated cyclic compressive load patterns capable of causing displacement or rupture of knee structures, such as tibial displacement and anterior cruciate ligament (ACL) rupture. Evidence from animal studies further indicates that joint immobilization not only induces KOA but also contributes to articular degeneration and delays healing.<sup>116</sup> In contrast, the effects of running appear to be contradictory. Short-term running has not been associated with radiological signs of KOA and may exert a protective effect.<sup>117</sup> whereas our findings suggest that running can induce osteoarthritis under conditions of excessive intensity or mechanical stress. Mechanical studies demonstrated that osteophyte formation occurred between

2 days and 32 weeks after intervention, depending on the species and the specific induction mechanism. Follow-up assessment time points varied widely across studies, ranging from immediately after intervention to 1 year post-intervention. Overall, mechanical induction methods are considered effective for KOA modeling due to their noninvasive nature, accessibility, and relatively low cost.

Genetic alterations typically induce early inflammatory changes that subsequently lead to joint structural deformation and the development of KOA. Alterations in bone structure and surrounding tissues may also accompany these changes.<sup>83</sup> McCoy et al. and Gregory et al. reported that genetically modified mouse models are relatively easy to generate and are valuable for investigating genetic factors involved in KOA pathogenesis, particularly genes associated with cartilage inflammation, degeneration, and bone remodeling.<sup>118-120</sup> The timing of post-intervention assessment checkpoints in genetic models ranged from birth to 25 months following genetic modification. Studies examining genetic models of osteoarthritis reported that osteophyte formation typically required 3 to 16 months. Genetic models that identify genes implicated in KOA pathogenesis hold promise for advancing gene-based and targeted therapeutic strategies;<sup>121</sup> however, substantial additional research is required to further elucidate these mechanisms and their translational potential.

Most surgical methods for inducing KOA within a short time frame are based on joint destabilization, primarily targeting injury to key knee stabilizing structures. Bendele et al. reported that surgical induction models in rats are advantageous because of their low incidence of postoperative infections.<sup>122</sup> Moreover, rats are generally more suitable for surgical procedures than mice because of their larger body size.<sup>123</sup> However, using genetically manipulated strains (e.g., knockdown and knockout models) is considerably more challenging in rats. As expected, models employing combined surgical procedures, such as anterior cruciate ligament and medial meniscus injury, exhibit more rapid and pronounced KOA progression.<sup>36,124</sup> In addition, surgical methods are frequently combined with other induction approaches and are commonly used as reference models for comparison with newly proposed techniques. Across the reviewed studies, post-intervention assessment checkpoints varied widely, ranging from 2 days to 16 months. Depending on the specific surgical intervention, the time required for osteophyte formation ranged from 1 to 16 weeks.

Initially, collagenase, papain, and hydrogen peroxide (H<sub>2</sub>O<sub>2</sub>) were used to chemically induce KOA; however, in subsequent years, monosodium iodoacetate (MIA) models were introduced as a less invasive approach. MIA inhibits glyceraldehyde-3-phosphate dehydrogenase-mediated glycolysis, leading to chondrocyte death.<sup>125,126</sup> This process

results in the loss of the proteoglycan matrix and the development of cartilage lesions. Across chemically induced models, the time required for osteophyte formation ranged from 1 to 12 weeks. Post-intervention assessment time points reported in studies investigating chemical induction methods varied widely, from 1 hour to 10 months. Chemical models appear to be particularly suitable for short-term follow-up studies and for analyzing the early initiation of KOA. Although combinations of chemical and surgical induction methods have been proposed,<sup>127</sup> limited data are currently available to fully elucidate the strengths and limitations of these combined approaches.

### **Limitations**

Most of the included studies were single-center investigations that did not use randomization. Furthermore, substantial heterogeneity in reporting systems, follow-up durations, and animal models across KOA studies precluded the feasibility of a meta-analysis. Various scoring systems, including the OARSI histopathology grading system and the Mankin score, were used to characterize osteoarthritic changes. The lack of a standardized, consistent grading scale hindered direct comparisons among different KOA models. In addition, KOA progression is inherently nonlinear, and factors such as animal species, model selection, and housing conditions may influence disease outcomes and experimental results.

### **Conclusion**

Each approach offers specific advantages regarding osteophyte formation, histopathological features, and the time required for KOA development, thereby facilitating investigations into disease mechanisms and therapeutic interventions.

### **Acknowledgement**

N/A

**Authors Contribution:** Authors who conceived and designed the analysis: Armin Arabzadeh – Mohammad Hossein nabian, Authors who collected the data: Armin Arabzadeh – Shervin Mossavarali – Kasra Mirzaei - Gita Manzari Tavakoli - Ayda Manzari Tavakoli, Authors who contributed data or analysis tools: Brian T. Feeley, Authors who performed the analysis: Ayda Manzari Tavakoli, Authors who wrote the paper: Armin Arabzadeh – Shervin Mossavarali – Kasra Mirzaei - Gita Manzari Tavakoli – Brian T.Feeley - Mohammad Hossein nabian, Other contribution: All authors read and approved the final version of the manuscript.

**Declaration of Conflict of Interest:** None of the authors have identified a conflict of interest.

**Declaration of Funding:** There was no funding source for this study.

**Declaration of Ethical Approval for Study:** No patients or

human subject are included in this study. The data that support the findings of this study are available on request from the corresponding author. The data are not publicly available due to privacy or ethical restrictions.

**Declaration of Informed Consent:** N/A

Armin Arabzadeh MD<sup>1,2</sup>  
Shervin Mossavarali MD<sup>1,2</sup>  
Gita Manzari Tavakoli MD<sup>3</sup>  
Kasra Mirzaei MD<sup>1,2</sup>  
Ayda Manzari Tavakoli MD<sup>3</sup>  
Brian T. Feeley MD<sup>4</sup>  
Mohammad Hossein Nabian MD<sup>1,5</sup>

1 Center for Orthopedic Trans-Disciplinary Applied Research, Tehran University of Medical Sciences, Tehran, Iran  
2 School of Medicine, Tehran University of Medical Sciences, Tehran, Iran  
3 Pediatric Urology and Regenerative Medicine Research Center, Children's Medical Center, Gene, Cell & Tissue Research Institute, Tehran University of Medical Sciences, Tehran, Iran  
4 Department of Orthopedic Surgery, University of California, San Francisco, 1500 Owens Street, San Francisco, CA, USA  
5 Department of Orthopedics, School of Medicine, Tehran University of Medical Sciences, Tehran, Iran

## References

- Hunter DJ, March L, Chew M. Osteoarthritis in 2020 and beyond: a Lancet Commission. *The Lancet*. 2020;396(10264):1711-1712. doi: 10.1016/S0140-6736(20)32230-3.
- Cui A, Li H, Wang D, Zhong J, Chen Y, Lu H. Global, regional prevalence, incidence and risk factors of knee osteoarthritis in population-based studies. *EclinicalMedicine*. Dec 2020;29-30:100587. doi:10.1016/j.eclinm.2020.100587
- Steinmetz JD, Culbreth GT, Haile LM, et al. Global, regional, and national burden of osteoarthritis, 1990&#x2013;2020 and projections to 2050: a systematic analysis for the Global Burden of Disease Study 2021. *The Lancet Rheumatology*. 2023;5(9):e508-e522. doi:10.1016/S2665-9913(23)00163-7
- Szponder T, Latalski M, Danielewicz A, et al. Osteoarthritis: Pathogenesis, Animal Models, and New Regenerative Therapies. *J Clin Med*. 2022;12(1)doi:10.3390/jcm12010005
- Kuyinu EL, Narayanan G, Nair LS, Laurencin CT. Animal models of osteoarthritis: classification, update, and measurement of outcomes. *J Orthop Surg Res*. Feb 2 2016;11:19. doi:10.1186/s13018-016-0346-5
- Cope PJ, Ourradi K, Li Y, Sharif M. Models of osteoarthritis: the good, the bad, and the promising. *Osteoarthritis Cartilage*. 2019;27(2):230-239. doi:10.1016/j.joca.2018.09.016
- Esdaille CJ, Ude CC, Laurencin CT. Regenerative Engineering Animal Models for Knee Osteoarthritis. *Regen Eng Transl Med*. 2022;8(2):284-297. doi:10.1007/s40883-021-00225-y
- Song X, Liu Y, Chen S, et al. Knee osteoarthritis: A review of animal models and intervention of traditional Chinese medicine. *Animal Models and Experimental Medicine*. 2024;7(2):114-126. doi: 10.1002/ame2.12389.
- Bendele AM, Hulman JF. Effects of Body Weight Restriction on the Development and Progression of Spontaneous Osteoarthritis in Guinea Pigs. Article. *Arthritis Rheum*. 1991;34(9):1180-1184. doi:10.1002/art.1780340916
- Go EJ, Kim SA, Cho ML, Lee KS, Shetty AA, Kim SJ. A Combination of Surgical and Chemical Induction in a Rabbit Model for Osteoarthritis of the Knee. *Tissue Eng Regen Med*. 2022;19(6):1377-1388. doi:10.1007/s13770-022-00488-8
- Liu Z, Hu X, Man Z, Zhang J, Jiang Y, Ao Y. A novel rabbit model of early osteoarthritis exhibits gradual cartilage degeneration after medial collateral ligament transection outside the joint capsule. *Sci Rep*. 2016;6:34423. doi:10.1038/srep34423
- Meacock SCR, Bodmer JL, Billingham MEJ. Experimental osteoarthritis in guinea-pigs. Article. *Journal of Experimental Pathology*. 1990;71(2):279-293.
- Glasson SS, Blanchet TJ, Morris EA. The surgical destabilization of the medial meniscus (DMM) model of osteoarthritis in the 129/SvEv mouse. *Osteoarthritis and Cartilage*. 2007;15(9):1061-1069. doi:10.1016/j.joca.2007.03.006
- Venne G, Tse MY, Pang SC, Ellis RE. Mechanically-induced osteophyte in the rat knee. *Osteoarthritis Cartilage*. 2020;28(6):853-864. doi:10.1016/j.joca.2020.02.834
- Langenskiöld A, Michelsson JE, Videman T. Osteoarthritis of the knee in the rabbit produced by immobilization: Attempts to achieve a reproducible model for studies on pathogenesis and therapy. Article. *Acta Orthopaedica*. 1979;50(1):1-14. doi:10.3109/17453677909024083
- Beckett J, Jin W, Schultz M, et al. Excessive running induces cartilage degeneration in knee joints and alters gait

of rats. *Journal of Orthopaedic Research*. 2012;30(10):1604-1610. doi:10.1002/jor.22124

17. Son KM, Jung HA, Hong JI, Park IY, Kim HA. Development of a Mouse Model of Knee Osteoarthritis Based on Obesity and Bipedal Walking. Article. *Journal of Orthopaedic Research*. 2019;37(11):2411-2419. doi:10.1002/jor.24411

18. Kaiki G, Tsuji H, Yonezawa T, et al. Osteoarthrosis induced by intra-articular hydrogen peroxide injection and running load. Article. *Journal of Orthopaedic Research*. 1990;8(5):731-740. doi:10.1002/jor.1100080515

19. Van Der Kraan PM, Vitters EL, Van Beuningen HM, Van De Putte LBA, Van Den Berg WB. Degenerative knee joint lesions in mice after a single intra-articular collagenase injection. A new model of osteoarthritis. Article. *Van Der Kraan PM, Vitters EL, Van Beuningen HM, Van De Putte LBA, Van Den Berg WB. Degenerative knee joint lesions in mice after a single intra-articular collagenase injection. A new model of osteoarthritis. Article. J Exp Pathol*. 1990;71(1):19-31.

20. Wang Z, Zheng C, Zhong Y, et al. Interleukin-17 can induce osteoarthritis in rabbit knee joints similar to hult's method. Article. *BioMed Research International*. 2017;2017:2091325. doi:10.1155/2017/2091325

21. Kopp S, Mejersjö C, Clemensson E. Induction of osteoarthrosis in the guinea pig knee by papain. Article. *Oral Surg Oral Med Oral Pathol*. 1983;55(3):259-266. doi:10.1016/0030-4220(83)90325-0

22. Boudierlique T, Vuppalapati KK, Newton PT, Li L, Barenus B, Chagin AS. Targeted deletion of Atg5 in chondrocytes promotes age-related osteoarthritis. Article. *Annals of the Rheumatic Diseases*. 2016;75(3):627-631. doi:10.1136/annrheumdis-2015-207742

23. Gilbert SJ, Meakin LB, Bonnet CS, et al. Deletion of P58IPK, the cellular inhibitor of the protein kinases PKR and PERK, causes bone changes and joint degeneration in mice. Article. *Frontiers in Endocrinology*. 2014;5:174. doi:10.3389/fendo.2014.00174

24. Song X, Liu Y, Chen S, et al. Knee osteoarthritis: A review of animal models and intervention of traditional Chinese medicine. *Animal Model Exp Med*. 2024;7(2):114-126. doi:10.1002/ame2.12389

25. Longo UG, Papalia R, De Salvatore S, Picozzi R, Sarubbi A, Denaro V. Induced Models of Osteoarthritis in Animal Models: A Systematic Review. *Biology (Basel)*. 2023;12(2)doi:10.3390/biology12020283

26. Moher D, Liberati A, Tetzlaff J, Altman DG. Preferred reporting items for systematic reviews and meta-analyses: the PRISMA statement. *PLoS medicine*. 2009;6(7):e1000097. doi:10.1371/journal.pmed.1000097

27. Sterne JAC, Savović J, Page MJ, et al. RoB 2: a revised tool for assessing risk of bias in randomised trials. *Bmj*. 2019;366:l4898. doi:10.1136/bmj.l4898

28. McGuinness LA, Higgins JPT. Risk-of-bias VISualization (robvis): An R package and Shiny web app for visualizing risk-of-bias assessments. *Res Synth Methods*. 2021;12(1):55-61. doi:10.1002/jrsm.1411

29. Dzidzishvili L, López T II, Guerrero CC, Calvo E. Developing an experimental model of early knee osteoarthritis after medial meniscus posterior root release: an in vivo study. *J Exp Orthop*. 2022;9(1):66. doi:10.1186/s40634-022-00501-y

30. Papaioannou N, Krallis N, Triantafillopoulos I, Khaldi L, Dontas I, Lyritis G. Optimal timing of research after anterior cruciate ligament resection in rabbits. *Contemp Top Lab Anim Sci*. 2004;43(6):22-7; quiz 58.

31. Kim JE, Song DH, Kim SH, Jung Y, Kim SJ. Development and characterization of various osteoarthritis models for tissue engineering. *Plos One*. 2018;13(3)e0194288. doi:10.1371/journal.pone.0194288

32. Tawonsawatruk T, Sriwatananukulkit O, Himakhun W, Hemstapat W. Comparison of pain behaviour and osteoarthritis progression between anterior cruciate ligament transection and osteochondral injury in rat models. *Bone & Joint Research*. 2018;7(3):244-251. doi:10.1302/2046-3758.73.Bjr-2017-0121.R2

33. Temp J, Labuz D, Negrete R, Sunkara V, Machelska H. Pain and knee damage in male and female mice in the medial meniscal transection-induced osteoarthritis. *Osteoarthritis and Cartilage*. 2020;28(4):475-485. doi:10.1016/j.joca.2019.11.003

34. Hu W, Lin J, Wei J, et al. Modelling osteoarthritis in mice via surgical destabilization of the medial meniscus with or without a stereomicroscope. Article. *Bone and Joint Research*. 2022;11(8):518-527. doi:10.1302/2046-3758.118.BJR-2021-0575.R1

35. Nukuto K, Matsushita T, Kamada K, et al. Development and Analysis of Mouse Medial Meniscus Posterior Root Tear Model. Article. *Calcified Tissue International*. 2023;112(1):55-65. doi:10.1007/s00223-022-01028-1

36. Pucha KA, McKinney JM, Fuller JM, Willett NJ. Characterization of OA development between sexes in the rat medial meniscal transection model. Article. *Osteoarthritis and Cartilage Open*. 2020;2(3)100066. doi:10.1016/j.ocarto.2020.100066

37. Appleton CTG, McErlain DD, Pitelka V, et al. Forced mobilization accelerates pathogenesis: Characterization of a preclinical surgical model of osteoarthritis. Article. *Arthritis Research and Therapy*. 2007;9910R13. doi:10.1186/ar2120

38. Bove SE, Laemont KD, Brooker RM, et al. Surgically induced osteoarthritis in the rat results in the development of both osteoarthritis-like joint pain and secondary hyperalgesia. Article. *Osteoarthritis and Cartilage*. 2006;14(10):1041-1048. doi:10.1016/j.joca.2006.05.001

39. Colombo C, Butler M, O'Byrne E, et al. A new model of osteoarthritis in rabbits. Article. *Arthritis & Rheumatism*. 1983;26(7):875-886. doi:10.1002/art.1780260709
40. Huebner KD, Shrive NG, Frank CB. New surgical model of post-traumatic osteoarthritis: Isolated intra-articular bone injury in the rabbit. Article. *Journal of Orthopaedic Research*. 2013;31(6):914-920. doi:10.1002/jor.22284
41. Kamekura S, Hoshi K, Shimoaka T, et al. Osteoarthritis development in novel experimental mouse models induced by knee joint instability. Article. *Osteoarthritis and Cartilage*. 2005;13(7):632-641. doi:10.1016/j.joca.2005.03.004
42. Karahan S, Kincaid SA, Kammermann JR, Wright JC. Evaluation of the rat stifle joint after transection of the cranial cruciate ligament and partial medial meniscectomy. Article. *Comparative Medicine*. 2001;51(6):504-512.
43. Lukoschek M, Schaffler MB, Burr DB, Boyd RD, Radin EL. Synovial membrane and cartilage changes in experimental osteoarthrosis. Article. *Journal of Orthopaedic Research*. 1988;6(4):475-492. doi:10.1002/jor.1100060403
44. McNulty MA, Loeser RF, Davey C, Callahan MF, Ferguson CM, Carlson CS. Histopathology of naturally occurring and surgically induced osteoarthritis in mice. Article. *Osteoarthritis and Cartilage*. 2012;20(8):949-956. doi:10.1016/j.joca.2012.05.001
45. Iijima H, Aoyama T, Ito A, et al. Destabilization of the medial meniscus leads to subchondral bone defects and site-specific cartilage degeneration in an experimental rat model. Article. *Osteoarthritis and Cartilage*. 2014;22(7):1036-1043. doi:10.1016/j.joca.2014.05.009
46. David MA, Smith MK, Pilachowski RN, White AT, Locke RC, Price C. Early, focal changes in cartilage cellularity and structure following surgically induced meniscal destabilization in the mouse. Article. *Journal of Orthopaedic Research*. 2017;35(3):537-547. doi:10.1002/jor.23443
47. Lefkoe TP, Trafton PG, Ehrlich MG, et al. An experimental model of femoral condylar defect leading to osteoarthrosis. *J Orthop Trauma*. 1993;7(5):458-67. doi:10.1097/00005131-199310000-00009
48. Piskin A, Gulbabar MY, Tomak Y, et al. Osteoarthritis models after anterior cruciate ligament resection and medial meniscectomy in rats: A histological and immunohistochemical study. Article. *Saudi Medical Journal*. 2007;28(12):1796-1802.
49. Shapiro F, Glimcher MJ. Induction of osteoarthrosis in the rabbit knee joint: Histologic changes following meniscectomy and meniscal lesions. Article. *Clinical Orthopaedics and Related Research*. 1980;(147):287-295.
50. Huang K, Cai HL, Zhang PL, Wu LD. Comparison between two rabbit models of posttraumatic osteoarthritis: A longitudinal tear in the medial meniscus and anterior cruciate ligament transection. *J Orthop Res*. 2020;38(12):2721-2730. doi:10.1002/jor.24645
51. Zahoor T, Mitchell R, Bhasin P, Schon L, Zhang Z. A Surgical Model of Posttraumatic Osteoarthritis With Histological and Gait Validation. Article. *Orthopaedic Journal of Sports Medicine*. 2016;4(7) doi:10.1177/2325967116658874
52. McCulloch K, Huesa C, Dunning L, et al. Accelerated post traumatic osteoarthritis in a dual injury murine model. Article. *Osteoarthritis and Cartilage*. 2019;27(12):1800-1810. doi:10.1016/j.joca.2019.05.027
53. Garcia F, Mitrovic DR. Joint reaction to polyethylene implantation: A method for inducing osteoarthritic change and osteophyte formation in the rabbit knee joint. Article. *Journal of Orthopaedic Research*. 1986;4(4):420-426. doi:10.1002/jor.1100040404
54. Stoop R, Buma P, Van Der Kraan P, et al. Type II collagen degradation in articular cartilage fibrillation after anterior cruciate ligament transection in rats. *Osteoarthritis and cartilage*. 2001;9(4):308-315. doi: 10.1053/joca.2000.0390
55. Hamilton C, Pest M, Pitelka V, Ratneswaran A, Beier F, Chesworth B. Weight-bearing asymmetry and vertical activity differences in a rat model of post-traumatic knee osteoarthritis. *Osteoarthritis and cartilage*. 2015;23(7):1178-1185. doi: 10.1016/j.joca.2015.03.001
56. Hayami T, Pickarski M, Zhuo Y, Wesolowski GA, Rodan GA, Duong LT. Characterization of articular cartilage and subchondral bone changes in the rat anterior cruciate ligament transection and meniscectomized models of osteoarthritis. *Bone*. 2006;38(2):234-243. doi: 10.1016/j.bone.2005.08.007
57. Maerz T, Newton M, Kurdziel M, et al. Articular cartilage degeneration following anterior cruciate ligament injury: a comparison of surgical transection and noninvasive rupture as preclinical models of post-traumatic osteoarthritis. *Osteoarthritis and cartilage*. 2016;24(11):1918-1927.
58. Rogart J, Barrach H-J, Chichester C. Articular collagen degradation in the Hulth-Telhag model of osteoarthritis. *Osteoarthritis and Cartilage*. 1999;7(6):539-547. doi: 10.1053/joca.1999.0258
59. Hulth A, Lindberg L, Telhag H. Experimental osteoarthritis in rabbits: preliminary report. *Acta Orthop Scand*. 1970;41(5):522-530. doi: 10.3109/17453677008991540
60. Rebai MA, Sahnoun N, Abdelhedi O, et al. Animal models of osteoarthritis: characterization of a model induced by Mono-Iodo-Acetate injected in rabbits. *Libyan J Med*. Dec 2020;15(1):1753943. doi:10.1080/19932820.2020.1753943
61. Park J, Lee J, Kim KI, et al. A Pathophysiological Validation of Collagenase II-Induced Biochemical Osteoarthritis Animal Model in Rabbit. *Tissue Eng Regen Med*. Aug 2018;15(4):437-444. doi:10.1007/s13770-018-0124-z

62. Vinod E, Boopalan P, Arumugam S, Sathishkumar S. Creation of monosodium iodoacetate-induced model of osteoarthritis in rabbit knee joint. *Indian J Med Res.* 2018;147(3):312-314. doi:10.4103/ijmr.IJMR\_2004\_16
63. Takahashi I, Matsuzaki T, Kuroki H, Hosono M. Induction of osteoarthritis by injecting monosodium iodoacetate into the patellofemoral joint of an experimental rat model. *Plos One.* 2018;13(4):e0196625. doi:10.1371/journal.pone.0196625
64. Okamoto M, Atsuta Y. Cartilage degeneration is associated with augmented chemically-induced joint pain in rats. Article. *Clinical Orthopaedics and Related Research.* 2010;468(5):1423-1427. doi:10.1007/s11999-009-1193-z
65. Adaes S, Mendonça M, Santos TN, Castro-Lopes JM, Ferreira-Gomes J, Neto FL. Intra-articular injection of collagenase in the knee of rats as an alternative model to study nociception associated with osteoarthritis. *Arthritis Research & Therapy.* 2014;16(1):R10. doi:10.1186/ar4436
66. Guingamp C, Gegout-Pottie P, Philippe L, Terlain B, Netter P, Gillet P. Mono-iodoacetate-induced experimental osteoarthritis: A dose-response study of loss of mobility, morphology, and biochemistry. Article. *Arthritis and Rheumatism.* 1997;40(9):1670-1679. doi:10.1002/art.1780400917
67. Barve RA, Minnerly JC, Weiss DJ, et al. Transcriptional profiling and pathway analysis of monosodium iodoacetate-induced experimental osteoarthritis in rats: relevance to human disease. *Osteoarthritis Cartilage.* 2007;15(10):1190-8. doi:10.1016/j.joca.2007.03.014
68. Yamada EF, Salgueiro AF, Goulart ADS, et al. Evaluation of monosodium iodoacetate dosage to induce knee osteoarthritis: Relation with oxidative stress and pain. Article. *International Journal of Rheumatic Diseases.* 2019;22(3):399-410. doi:10.1111/1756-185X.13450
69. Van der Kraan PM, Vitters EL, Van de Putte LBA, Van den Berg WB. Development of osteoarthritic lesions in mice by 'metabolic' and 'mechanical' alterations in the knee joints. Article. *American Journal of Pathology.* 1989;135(6):1001-1014.
70. Borella L, Eng CP, DiJoseph J, et al. Rapid induction of early osteoarthritic-like lesions in the rabbit knee by continuous intra-articular infusion of mammalian collagenase or interleukin-1. Article. *Agents and Actions.* 1991;34(1-2):220-222. doi:10.1007/BF01993285
71. Li F, Yin Z, Wu H, Qin Z, Li Z, Qiu Y. Section of the anterior cruciate ligament in the rabbit as animal model for osteoarthritis progression. *Int Orthop.* 2016;40(2):407-16. doi:10.1007/s00264-015-2854-z
72. Zhang YW, Su YL, Lanning N, et al. Targeted disruption of *Mig-6* in the mouse genome leads to early onset degenerative joint disease. *Proceedings of the National Academy of Sciences of the United States of America.* 2005;102(33):11740-11745. doi:10.1073/pnas.0505171102
73. Bellini M, Pest MA, Miranda-Rodrigues M, Qin L, Jeong JW, Beier F. Overexpression of MIG-6 in the cartilage induces an osteoarthritis-like phenotype in mice. Article. *Arthritis Research and Therapy.* 2020;22(1):119. doi:10.1186/s13075-020-02213-z
74. Qu M, Chen M, Gong W, et al. Pip5k1c Loss in Chondrocytes Causes Spontaneous Osteoarthritic Lesions in Aged Mice. Article. *Aging and Disease.* 2023;14(2):502-514. doi:10.14336/AD.2022.0828
75. Rellmann Y, Eidhof E, Hansen U, et al. Er stress in erp57 knockout knee joint chondrocytes induces osteoarthritic cartilage degradation and osteophyte formation. Article. *International Journal of Molecular Sciences.* 2021;23(1):182. doi:10.3390/ijms23010182
76. Bomsta BD, Bridgewater LC, Seegmiller RE. Premature osteoarthritis in the Disproportionate micromelia (Dmm) mouse. Article. *Osteoarthritis and Cartilage.* 2006;14(5):477-485. doi:10.1016/j.joca.2005.11.011
77. Lapveteläinen T, Hyttinen M, Lindblom J, et al. More knee joint osteoarthritis (OA) in mice after inactivation of one allele of type II procollagen gene but less OA after lifelong voluntary wheel running exercise. Article. *Osteoarthritis and Cartilage.* 2001;9(2):152-160. doi:10.1053/joca.2000.0370
78. Masuya H, Nishida K, Furuichi T, et al. A novel dominant-negative mutation in *Gdf5* generated by ENU mutagenesis impairs joint formation and causes osteoarthritis in mice. Article. *Human Molecular Genetics.* 2007;16(19):2366-2375. doi:10.1093/hmg/ddm195
79. Wu Q, Kim KO, Sampson ER, et al. Induction of an osteoarthritis-like phenotype and degradation of phosphorylated Smad3 by Smurf2 in transgenic mice. Article. *Arthritis and Rheumatism.* 2008;58(10):3132-3144. doi:10.1002/art.23946
80. Yuan G, Xu L, Cai T, et al. Clock mutant promotes osteoarthritis by inhibiting the acetylation of NFκB. Article. *Osteoarthritis and Cartilage.* 2019;27(6):922-931. doi:10.1016/j.joca.2019.01.012
81. Cornelis FMF, de Roover A, Storms L, Hens A, Lories RJ, Monteagudo S. Increased susceptibility to develop spontaneous and post-traumatic osteoarthritis in *Dot1l*-deficient mice. Article. *Osteoarthritis and Cartilage.* 2019;27(3):513-525. doi:10.1016/j.joca.2018.11.008
82. Wang Q, Tan QY, Xu W, et al. Cartilage-specific deletion of *Alk5* gene results in a progressive osteoarthritis-like phenotype in mice. Article. *Osteoarthritis and Cartilage.* 2017;25(11):1868-1879. doi:10.1016/j.joca.2017.07.010
83. Valverde-Franco G, Lussier B, Hum D, et al. Cartilage-specific deletion of ephrin-B2 in mice results in early developmental defects and an osteoarthritis-like phenotype during aging in vivo. Article. *Arthritis Research and Therapy.* 2016;18(1):65. doi:10.1186/S13075-016-0965-6
84. Stiffel V, Rundle CH, Sheng MH, Das S, Lau KW. A Mouse Noninvasive Intraarticular Tibial Plateau Compression

Loading-Induced Injury Model of Posttraumatic Osteoarthritis. *Calcif Tissue Int.* 2020;106(2):158-171. doi:10.1007/s00223-019-00614-0

85. Langenskiöld A, Michelsson JE, Videman T. Osteoarthritis of the knee in the rabbit produced by immobilization. Attempts to achieve a reproducible model for studies on pathogenesis and therapy. *Acta Orthop Scand.* 1979;50(1):1-14. doi:10.3109/17453677909024083

86. Brown SB, Hornyak JA, Jungels RR, et al. Characterization of Post-Traumatic Osteoarthritis in Rats Following Anterior Cruciate Ligament Rupture by Non-Invasive Knee Injury (NIKI). *J Orthop Res.* 2020;38(2):356-367. doi:10.1002/jor.24470

87. Horisberger M, Fortuna R, Valderrabano V, Herzog W. Long-term repetitive mechanical loading of the knee joint by in vivo muscle stimulation accelerates cartilage degeneration and increases chondrocyte death in a rabbit model. *Clinical Biomechanics.* 2013;28(5):536-543. doi:10.1016/j.clinbiomech.2013.04.009

88. Timkovich AE, Sikes KJ, Andrie KM, et al. Full and Partial Mid-substance ACL Rupture Using Mechanical Tibial Displacement in Male and Female Mice. *Annals of Biomedical Engineering.* 2023;51(3):579-593. doi:10.1007/s10439-022-03065-1

89. Wu P, Holguin N, Silva MJ, Fu M, Liao W, Sandell LJ. Early response of mouse joint tissue to noninvasive knee injury suggests treatment targets. Article. *Arthritis Rheum.* 2014;66(5):1256-1265. doi:10.1002/art.38375

90. Ko FC, Dragomir C, Plumb DA, et al. In vivo cyclic compression causes cartilage degeneration and subchondral bone changes in mouse tibiae. Article. *Arthritis and Rheumatism.* 2013;65(6):1569-1578. doi:10.1002/art.37906

91. Poulet B, Westerhof TAT, Hamilton RW, Shefelbine SJ, Pitsillides AA. Spontaneous osteoarthritis in Str/ort mice is unlikely due to greater vulnerability to mechanical trauma. Article. *Osteoarthritis and Cartilage.* 2013;21(5):756-763. doi:10.1016/j.joca.2013.02.652

92. Pap G, Eberhardt R, Stürmer I, et al. Development of osteoarthritis in the knee joints of Wistar rats after strenuous running exercise in a running wheel by intracranial self-stimulation. Article. *Pathology Research and Practice.* 1998;194(1):41-47. doi:10.1016/S0344-0338(98)80010-1

93. Ramos-Mucci L, Elsheikh A, Keenan C, et al. The anterior cruciate ligament in murine post-traumatic osteoarthritis: markers and mechanics. Article. *Arthritis Research and Therapy.* 2022;24(1):128. doi:10.1186/s13075-022-02798-7

94. Zhao Z, Ito A, Nakahata A, et al. One session of 20 N cyclic compression induces chronic knee osteoarthritis in rats: A long-term study. Article. *Osteoarthritis and Cartilage Open.* 2022;4(4):100325. doi:10.1016/j.ocarto.2022.100325

95. Beckett J, Jin W, Schultz M, et al. Excessive running induces cartilage degeneration in knee joints and alters gait of rats. Article. *Journal of Orthopaedic Research.* 2012;30(10):1604-1610. doi:10.1002/jor.22124

96. Poulet B, Hamilton RW, Shefelbine S, Pitsillides AA. Characterizing a novel and adjustable noninvasive murine joint loading model. Article. *Arthritis and Rheumatism.* 2011;63(1):137-147. doi:10.1002/art.27765

97. Radin EL, Martin RB, Burr DB, Caterson B, Boyd RD, Goodwin C. Effects of mechanical loading on the tissues of the rabbit knee. Article. *Journal of Orthopaedic Research.* 1984;2(3):221-234. doi:10.1002/jor.1100020303

98. Roemhildt ML, Beynon BD, Gauthier AE, Gardner-Morse M, Ertem F, Badger GJ. Chronic in vivo load alteration induces degenerative changes in the rat tibiofemoral joint. *Osteoarthritis and Cartilage.* 2013;21(2):346-357. doi:10.1016/j.joca.2012.10.014

99. Videman T. Experimental osteoarthritis in the rabbit: Comparison of different periods of repeated immobilization. Article. *Acta Orthopaedica.* 1982;53(3):339-347. doi:10.3109/17453678208992226

100. Poulet B, de Souza R, Kent AV, et al. Intermittent applied mechanical loading induces subchondral bone thickening that may be intensified locally by contiguous articular cartilage lesions. Article. *Osteoarthritis and Cartilage.* 2015;23(6):940-948. doi:10.1016/j.joca.2015.01.012

101. Ji X, Ito A, Nakahata A, Nishitani K, Kuroki H, Aoyama T. Effects of in vivo cyclic compressive loading on the distribution of local Col2 and superficial lubricin in rat knee cartilage. *Journal of Orthopaedic Research®.* 2021;39(3):543-552. doi: 10.1002/jor.24812

102. de Visser HM, Mastbergen SC, Kozijn AE, et al. Metabolic dysregulation accelerates injury-induced joint degeneration, driven by local inflammation; an in vivo rat study. *J Orthop Res.* 2018;36(3):881-890. doi:10.1002/jor.23712

103. Ernest TL, Kondrashov PE. The role of excessive body weight and meniscal instability in the progression of osteoarthritis in a rat model. *Knee.* 2018;25(6):1151-1156. doi:10.1016/j.knee.2018.07.009

104. Warmink K, Kozijn AE, Bobeldijk I, Stoop R, Weinans H, Korthagen NM. High-fat feeding primes the mouse knee joint to develop osteoarthritis and pathologic infrapatellar fat pad changes after surgically induced injury. *Osteoarthritis Cartilage.* 2020;28(5):593-602. doi:10.1016/j.joca.2020.03.008

105. Warmink K, Rios JL, van Valkengoed DR, Korthagen NM, Weinans H. Sprague Dawley Rats Show More Severe Bone Loss, Osteophytosis and Inflammation Compared to Wistar Han Rats in a High-Fat, High-Sucrose Diet Model of Joint Damage. *International Journal of Molecular Sciences.* 2022;23(7):3725. doi:10.3390/ijms23073725

106. Griffin TM, Huebner JL, Kraus VB, Yan Z, Guilak F. Induction of osteoarthritis and metabolic inflammation by a very high-fat diet in mice: Effects of short-term exercise. Article. *Arthritis and Rheumatism*. 2012;64(2):443-453. doi:10.1002/art.33332
107. Sulaiman SZS, Tan WM, Radzi R, et al. Comparison of bone and articular cartilage changes in osteoarthritis: a micro-computed tomography and histological study of surgically and chemically induced osteoarthritic rabbit models. *Journal of Orthopaedic Surgery and Research*. 2021;16(1)663. doi:10.1186/s13018-021-02781-z
108. Naveen SV, Ahmad RE, Hui WJ, et al. Histology, glycosaminoglycan level and cartilage stiffness in monoiodoacetate-induced osteoarthritis: comparative analysis with anterior cruciate ligament transection in rat model and human osteoarthritis. *International Journal of Medical Sciences*. 2013;11(1):97. doi: 10.7150/ijms.6964
109. Mapp P, Sagar D, Ashraf S, et al. Differences in structural and pain phenotypes in the sodium monoiodoacetate and meniscal transection models of osteoarthritis. *Osteoarthritis and Cartilage*. 2013;21(9):1336-1345. doi: 10.1016/j.joca.2013.06.031
110. Fernihough J, Gentry C, Malcangio M, et al. Pain related behaviour in two models of osteoarthritis in the rat knee. *Pain*. 2004;112(1-2):83-93. doi: 10.1016/j.pain.2004.08.004
111. Li C, He Y, Li Y, et al. A novel method to establish the rabbit model of knee osteoarthritis: intra-articular injection of SDF-1 induces OA. *BMC Musculoskelet Disord*. 3 2021;22(1):329. doi:10.1186/s12891-021-04188-7
112. Aüllo-Rasser G, Dousset E, Roffino S, et al. Early-stage knee OA induced by MIA and MMT compared in the murine model via histological and topographical approaches. *Scientific Reports*. 2020;10(1)15430. doi:10.1038/s41598-020-72350-7
113. Williams MD, Meyers RC, Braxton LA, Diekman B, X. Lascelles BD. Pilot comparison of outcome measures across chemical and surgical experimental models of chronic osteoarthritis in the rat (*Rattus norvegicus*). Article. *PLoS ONE*. 2022;17(11) e0277943. doi:10.1371/journal.pone.0277943
114. Yang Y, Li P, Zhu S, Bi R. Comparison of early-stage changes of osteoarthritis in cartilage and subchondral bone between two different rat models. Article. *PeerJ*. 2020;8 e8934. doi:10.7717/peerj.8934
115. Alexander PG, McCarron JA, Levine MJ, et al. An *In Vivo* Lapine Model for Impact-Induced Injury and Osteoarthritic Degeneration of Articular Cartilage. *Cartilage*. 2012;3(4):323-333. doi:10.1177/1947603512447301
116. Videman T. Experimental models of osteoarthritis: the role of immobilization. *Clin Biomech (Bristol, Avon)*. 1987;2(4):223-9. doi:10.1016/0268-0033(87)90086-6
117. Dhillon J, Kraeutler MJ, Belk JW, et al. Effects of Running on the Development of Knee Osteoarthritis: An Updated Systematic Review at Short-Term Follow-up. *Orthop J Sports Med*. 2023;11(3):23259671231152900. doi:10.1177/23259671231152900
118. McCoy A. Animal models of osteoarthritis: comparisons and key considerations. *Vet Pathol*. 2015;52(5):803-818. doi: 10.1177/0300985815588611
119. Gregory MH, Capito N, Kuroki K, Stoker AM, Cook JL, Sherman SL. A review of translational animal models for knee osteoarthritis. *Arthritis*. 2012;2012(1):764621..
120. Aydin M, Alp Avci G, Yilmaz UI, Aydin T, Avci E. Evaluation of Oxidative Stress and Cellular Immunity in Grades III-IV Knee Osteoarthritis. *The Archives of Bone and Joint Surgery*. 2024;12(12):840-845. doi:10.22038/abjs.2024.78412.3612
121. Evans CH, Ghivizzani SC, Robbins PD. Osteoarthritis gene therapy in 2022. *Curr Opin Rheumatol*. 2023;35(1):37-43. doi:10.1097/bor.0000000000000918
122. Bendele A. Animal models of osteoarthritis. *J Musculoskelet Neuronal Interact*. 2001;1(4):363-76.
123. Little CB, Smith MM. Animal models of osteoarthritis. Review. *Curr Rheumatol Rev*. 2008;4(3):175-182. doi:10.2174/157339708785133523
124. Hamilton CB, Pest MA, Pitelka V, Ratneswaran A, Beier F, Chesworth BM. Weight-bearing asymmetry and vertical activity differences in a rat model of post-traumatic knee osteoarthritis. *Osteoarthritis and Cartilage*. 2015;23(7):1178-1185. doi:10.1016/j.joca.2015.03.001
125. Morais SV, Czczeko NG, Malafaia O, et al. Osteoarthritis model induced by intra-articular monosodium iodoacetate in rats knee. *Acta Cir Bras*. 2016;31(11):765-773. doi:10.1590/s0102-865020160110000010
126. RODRIGUEZ-MERCHAN EC. The Current Role of Disease-modifying Osteoarthritis Drugs. *Arch Bone Jt Surg*. 2023;11(1):11-22. doi:10.22038/abjs.2021.56530.2807
127. Go EJ, Kim SA, Cho ML, Lee KS, Shetty AA, Kim SJ. A Combination of Surgical and Chemical Induction in a Rabbit Model for Osteoarthritis of the Knee. Article. *Tissue Engineering and Regenerative Medicine*. 2022;19(6):1377-1388. doi:10.1007/s13770-022-00488-8



Supplementary Table 1. Surgical models of knee osteoarthritis

Intervention	Animal	First author, year	Number of models	Sex	Age	Weight	Checkpoints after intervention	Osteophyte KOA score	KOA related findings	
ACLT	New Zealand white rabbits	Go, 2022 <sup>10</sup>	3	-	-	3500 ± 500 g	12 weeks	12 weeks	Modified Mankin Score: Femur: (3.78 ± 0.19), Tibia: (3.33 ± 0.33)	rough articular surface - osteophyte formation - cartilage loss - irregular cartilage surface - chondrocyte lost in full thickness - reduced alcian blue staining - fibrillation - matrix loss - chondrocyte hypertrophy - erosion - reduction of Collagen type II
		Liu, 2016 <sup>11</sup>	24	-	4-6 months old	2500 - 3000 g	1, 2, 3, 4, 5, 6 weeks (n=4 at each checkpoint)	-	irregular cartilage surface (since week 2) - rough articular surface (since week 3) - fibrillation (since week 3) - matrix loss (since week 4) - fissuring (since week 4) - significant higher MMP-1 level compared to sham group (since week 2) - significant higher MMP-13 level compared to sham group (at week 2 and 4) - cartilage degeneration (MRI T2 mapping values (statistically significant differences compared to sham group since week 3))	
		Papaioannou, 2004 <sup>30</sup>	15	Male	-	2045 ± 210 g	8 weeks (n=9) and 16 weeks (n=6)	8 weeks	rough articular surface (since week 8) - deep ulceration (since week 8) - osteophyte formation (since week 8) - cartilage loss (since week 8) - reduced Periodic acid-Schiff (PAS) staining (7 animals at week 8 and 4 animals at week 16) - reduced alcian blue staining (6 animals at week 8 and 3 animals at week 16) - subchondral cysts (since week 8)	
		Kim, 2018 <sup>31</sup>	5	Female	4 months	-	4 weeks	-	Modified Mankin Score: global Score: (11.8 ± 2.8)	rough articular surface - irregular cartilage surface - chondrocyte lost in full thickness - reduced alcian blue staining - cartilage loss - erosion - complete elimination of medial meniscus
		Sulaiman, 2021 <sup>107</sup>	15	Male	8-9 months	1800 - 2000 g	4,8,12 weeks (n=5 at each checkpoint)	-	OARSI Scoring System (median): week 4: (femur=0, Tibia=0), week 8: (femur=1, Tibia=0), week 12: (femur=1, Tibia=2)	sclerosis (at week 4 and 8, observed by micro-CT) - irregular cartilage surface (since week 4) - fibrillation (since week 4)
		Huang, 2020 <sup>50</sup>	15	Male	-	mean body weight: 3500 g, range: 2800 -	4,6,9 weeks (n=5 at each time point)	-	-	fibrosis (since week 4) - irregular cartilage surface (since week 4) - reduced safranin o-fast staining (since week 6) - superficial to middle cartilage ulceration (at week 6) - superficial fissures (at week 6) - partial-thickness cartilage erosion (at week 9) - reduction of Collagen type II and aggrecan (since week 6) - increased expression of IL-1β, MMP-3, MMP-13, ADAMTS-4, and ADAMTS-5 (since week 4)
		Piskin, 2006 <sup>48</sup>	24	Male	-	-	8,16 weeks (n=12 at each timepoint)	-	Modified Mankin Score: week 8: (femoral Condyles: (5.50 ± 3.50), Tibial Plateau: (2.50 ± 1.97)), week 16: (femoral Condyles: (7.72 ± 3.66), Tibial Plateau: (7.27 ± 3.13))	cartilage loss (since week 8) - irregular cartilage surface (since week 8) - reduced safranin o-fast staining (since week 8) - fibrillation (since week 8) - proteoglycan loss (since week 8) - increased expression of MMP13 (significant increases in MMP13 expression at week 8 postsurgery compared to week 16 (p<0.05))
	Hayami, 2005 <sup>56</sup>	-	Male	2.5 months	-	-	1,2,4,6,10 weeks	6 weeks	-	surface damage (since week 2) - fibrosis (since week 2) - fibrillation (since week 2) - irregular cartilage surface (since week 4) - proteoglycan loss (since week 4) - rough articular surface (since week 6) - osteophyte formation (since week 6) - loss of cellularity (since week 6) -



MMT	New Zealand white rabbits	Huang, 2020 <sup>50</sup>	15	Male	-	mean body weight: 3500 g, range: 2800 -	4,6,9 weeks (n=5 at each checkpoint)	-	-	-	-	-	fibrosis (since week 4) - ulceration (superficial to middle cartilage ulceration at week 9) - irregular cartilage surface (since week 4) - chondrocyte loss in full thickness (since week 4) - reduced safranin o-fast staining (since week 4) - increased expression of IL-1 $\beta$ , MMP-3, MMP-13, ADAMTS-4, and ADAMTS-5 (since week 4) - decreased expression of aggrecan and type II collagen (since week 4)		
		Piskin, 2006 <sup>48</sup>	24	Male	-	-	8,16 weeks (n=12 at each checkpoint)	-	-	-	-	-	Modified Mankin Score: week 8: (femoral Condyles: (7.16 $\pm$ 3.37), Tibial Plateau: (10.75 $\pm$ 4.39)), week 16: (femoral Condyles: (8.83 $\pm$ 5.56), Tibial Plateau: (8.33 $\pm$ 6.08))	cartilage loss (since week 8) - irregular cartilage surface (since week 8) - reduced stain of safranin o-fast (since week 8) - fibrillation (since week 8) - proteoglycan loss (since week 8) - increased expression of MMP13 (significant increases in MMP13 expression at week 8 postsurgery compared to week 16 (p<0.05)) - chondrocytes clustering (since week 8)	
		Aül	8	Male	-	3	5	4 weeks	-	-	-	-	-	Mankin score :3.8 $\pm$ 0.63	irregular cartilage surface
		Wistar rats	Iijima, 2014 <sup>45</sup>	24	Male	-	3 months old	1,2,4 weeks (n=8 at each checkpoint)	-	-	-	-	-	Modified OARSI scoring System: middle region ((week 1: 7.5(2.3-8.0), week 2: 12.0(7.5-13.1), week 4: 13.8(12.4-16.0) - outer Region: ((week 1: 3.0(2.0-3.0), week 2: 3.0(3.0-3.8), week 4: 4.0(3.3-6.0),)) - inner Region: ((week1: 1.0(0.3-1.0), week 2: 1.0(1.0-1.8), week 4: 1.0(1.0-5.5)))	fissure (since week 1) - matrix loss (since week 1) - fibrillation (since week 4) - subchondral bone defects (on micro-CT image at week 4) - fibrosis (at week 4) - increased expression of MMP13 (at week 4)
		129S6/SvEv mice	Glasson, 2007 <sup>13</sup>	at least 10	Male	-	-	4,8 weeks	-	-	-	-	-	A modified semiquantitative grading Scale: week 4: (maximum scores Method: (3.7 $\pm$ 1.5), summed score Method: (25.2 $\pm$ 4.7), week 8: (maximum scores Method: (4.1 +- 0.3), summed score Method: (35.7 +- 3.8)	cartilage loss (at week 8)- reduced stain of safranin o-fast (at week 8) - fibrillation (at week 8)
	Sprague Dawley rats	McCulloch, 2019 <sup>52</sup>	8	Male	2	2	22 - 28 g	1,2,4 weeks	-	-	-	-	-	synovitis (since week 2) - thickened synovial membrane (since week 2) - osteophyte formation (3 animals on week 1 and 6 animals on week 2, osteophyte BV/VT: p<0.01 compared to sham on week 2) - subchondral sclerosis (BV/VT: p<0.01 compared to sham on week 1)	
		David, 2017 <sup>46</sup>	-	Male	2	2	-	3 days and 1,2,8,12, 16 weeks (n=5-10)	-	-	-	-	-	fibrosis (since week 1) - cartilage loss (since week 1) - irregular cartilage surface (since week 1) - reduced safranin o-fast staining (since week 1) - fibrillation (since week 1) - erosion (since week 12) - proteoglycan loss (since week 1)	
		McNulty, 2012 <sup>44</sup>	12	Male	2	2	-	8 weeks	-	-	-	-	-	osteophyte formation (six axial osteophytes were identified; all were located on the lateral tibial plateau and were distributed evenly among surgical groups, six abaxial osteophytes were identified in the joints; all were located on the medial tibial plateaus of DMM stifles)	
		McNulty, 2012 <sup>44</sup>	8	Male	2	2	-	8 weeks	-	-	-	-	-	osteophyte formation (five axial osteophytes were present in the lateral tibial plateau and two in the medial tibial plateau and these were evenly divided between surgical groups, three abaxial osteophytes were present in the medial tibial plateau)	
		Total Mankin HHGS: 11.6 (10.9, 12.4)	-	-	-	-	-	-	-	-	-	-	-	osteophyte formation (five axial osteophytes were present in the lateral tibial plateau and two in the medial tibial plateau and these were evenly divided between surgical groups, three abaxial osteophytes were present in the medial tibial plateau)	

MCLT		MMPRT (medial meniscus posterior root transection)		MCLT + MMx		MMT + MCLT				MMx			
New Zealand white rabbits	Liu, 2016 <sup>11</sup>	C57Black6/J mice	New Zealand white rabbits	C57Black6/J mice	Sprague Dawley rats	Lewis rats	Lewis rats	Lewis rats	C57Black6/J mice	New Zealand white rabbits			
24	47	30	12	30	24	12	15	15	1	Shapiro, 1980 <sup>49</sup>			
-	-	-	-	-	Male	Male	Female	Male	Female	-			
4-6 months old	3 months old	2 months old	-	2 months old	-	-	-	-	2	12 months old			
2500 - 3000 g	-	18 - 22 g	approximately 2500 - 3000 g	18 - 22 g	approximately 180 g	200 - 225 g	275 - 300 g	300 - 350 g	-	-			
1,2,3,4,5,6 weeks (n=4 at each checkpoint)	2,4,8,12 weeks	2(n=7), 4(n=7), 8(n=7) and 12(n=9) weeks	16 weeks	2(n=7), 4(n=7), 8(n=7) and 12(n=9) weeks	2,5,7 weeks	3 weeks	3 weeks	3 weeks	1	8,28,40 weeks			
-	-	12 weeks	16 weeks	12 weeks	7 weeks	3 weeks	3	3	-	8 weeks			
			OARSI Scoring System (median interquartile Range): nonweight bearing area of medial Femur: 2(0.5), weight bearing area of medial Femur: 16(7), Medial Tibia: 6(3)		osteophyte Scores: day 49: (median: 2.0(IQR = 1.0-2.0), chondropathy Score: day 49: (median: 15 (IQR = 10-15)						Modified Mankin score (mean Grade): month 2: (3.5±1.6), month 7: (6.4±2.16), month 10: (7.1±2.12)		fibrosis (since week 8) - osteophyte formation (since week 8) - irregular cartilage surface (since week 8) - reduced safranin o-fast staining (since week 8) - fibrillation (since week 8) - fissure (since week 8) - cloning of chondrocytes (since week 8)
			Knee Joint space narrowing - rough articular surface - deep ulceration - osteophyte formation - cartilage loss - irregular cartilage surface - chondrocyte lost in full thickness - reduced safranin o-fast staining - fibrillation - synovitis - infiltration of subchondral bone - synovial hyperplasia - hemosiderin deposit										irregular cartilage surface
			deep ulceration (week 12) - irregular cartilage surface (week 8) - reduced safranin o-fast staining (week 2 and 4) - subchondral thickening (since week 8) - presence of Collagen type X (at week 8) - reduction of Collagen type II (at week 8) - increased expression of MMP13 (at week 8)										irregular cartilage surface
			fibrillation (since week 3) - rough articular surface (since week 3) - irregular cartilage surface (since week 3) - significant higher IL-6 level compared to sham group (at week 4 and 6) - significant higher MMP-1 level compared to sham group (at week 1 and 2) - significant higher MMP-13 level compared to sham group (at week 1,2,4,5 and 6) - cartilage degeneration (MRI T2 mapping values (statistically significant differences compared to sham group since week										osteophyte formation (along the medial edge of the tibiae) - rough articular surface - irregular cartilage surface - reduced safranin o-fast staining - fibrillation - proteoglycan loss
													osteophyte formation (along the medial edge of the tibiae) - rough articular surface - irregular cartilage surface - reduced safranin o-fast staining - fibrillation - proteoglycan loss
													fibrosis - osteophyte formation - cartilage loss - irregular cartilage surface - chondrocyte lost in full thickness - bone marrow fibrosis - subchondral sclerosis - erosion - proteoglycan loss



ACLT + PCLT + MCLT + MMx	ACLT + PCLT + MMT	ACLT + DMM	ACLT + MCLT + MMX	meniscal lesion	LCLT + MCLT	LCLT	MCLT + PMM
Japanese white	New Zealand white rabbits	Sprague Dawley	Sprague Dawley	New Zealand white rabbits	Olac guinea-pigs derived from a Dunkin Hartley	Olac guinea-pigs derived from a Dunkin Hartley	Meacock, 1990 <sup>12</sup>
Canzhang Li, 2021 <sup>111</sup>	Wang, 2017 <sup>20</sup>	Williams, 2022 <sup>113</sup>	Hayami, 2005 <sup>56</sup>	Shapiro, 1980 <sup>49</sup>	Meacock, 1990 <sup>12</sup>	Meacock, 1990 <sup>12</sup>	Meacock, 1990 <sup>12</sup>
9	15	6	-	16	30	-	-
-	-	Female	Male	-	Male	Male	Male
3	-	2 - 2.5	2.5 months old	12 months	-	-	-
2000 - 2500 g	approximately 2000 g	278 - 373 g	-	-	500 - 550 g	650 - 800 g	650 - 800 g
4,8,12 weeks	3 days and 1,3,6,12 weeks	6 weeks	1,2,4,6,10 weeks	12, 28, 64 weeks	3,5,7 weeks (n=10 at each checkpoint)	were examined at 2-week intervals between 2-7 weeks	1, 2, 3, 5, 7, 11, 16, 20, 25 weeks (Groups of 2 or 3 animals at each checkpoint)
12	6 weeks	-	6 weeks	12 weeks	-	-	7 weeks
-	-	-	-	Modified Mankin score (mean Grade): month 3: (4.8 ± 1.68), month 7: (5.2 ± 1.52), month 16: (6.0 ± 1.11)	-	-	-
-	-	-	-	fibrosis changes (since week 12) - osteophyte formation (since week 12 in 8 of 15 animals) - irregular cartilage surface (since week 12) - reduced safranin o-fast staining (since week 12) - fibrillation (since week 12) - fissure (since week 12) - chondrocyte cloning (since week 12)	-	-	osteophyte formation (since week 7) - cartilage loss (since week 1) - irregular cartilage surface (since week 1) - reduced alcian blue staining (at week 2,3,5 and 7) - fibrillation (at week 2,3,5,7 and 20) - subchondral cysts (at week 25) - thickened synovial membrane (at week 1) - synovial hyperplasia (at week 1) - synovium fibrosis (at week 1)
-	-	-	-	fibrosis changes (since week 2) - rough articular surface (since week 6) - osteophyte formation (since week 6) - irregular cartilage surface (since week 1) - fibrillation (since week 2) - significant increase in subchondral bone volume accompanied with decreased bone marrow area (at week 10) - bone eburnation (at week 6 and 10) - proteoglycan loss (since week 1) - cell clustering (since week 4) - loss of cellularity (since week 6)	-	-	cartilage loss (since week 6) - irregular cartilage surface (since week 6) - fibrillation (since week 10) - subchondral cysts (at week 30) - synovial hyperplasia - synovium fibrosis
-	-	-	-	-	-	-	cartilage loss (since week 3) - irregular cartilage surface (since week 3) - synovial hyperplasia - synovium fibrosis
-	-	-	-	-	-	-	irregular cartilage surface (week 4) - rough articular surface (week 8) - fissure (week 8) - osteophyte formation (week 12) - deep ulceration (week 8) - cartilage loss (week 8)
-	-	-	-	-	-	-	irregular cartilage surface (week 4) - rough articular surface (week 8) - fissure (week 8) - osteophyte formation (week 12) - deep ulceration (week 8) - cartilage loss (week 8)
-	-	-	-	-	-	-	irregular cartilage surface (week 4) - rough articular surface (week 8) - fissure (week 8) - osteophyte formation (week 12) - deep ulceration (week 8) - cartilage loss (week 8)

intra articular fracture of	introducing a plastic device into	femoral condyle injury <sup>c</sup>	cartilage scratch + DMM	cartilage scratch	osteophyte formation (3 of 8 animals on week 1, all animals on week 2, osteophyte BV/VT: compared to sham group on week 2: p<0.01) - subchondral sclerosis (compared to Sham on week 1: p<0.001) - synovitis (week 2)
Sprague-Dawley rats	New Zealand white rabbits	New Zealand white rabbits	C57Black6/1 mice	C57Black6/1 mice	osteophyte formation (6 of 8 animals on week 1, all animals on week 2, osteophyte number DCS compared to sham group on week 1: p<0.01, osteophyte BV/VT compared to sham group on week 2: p<0.001) - subchondral osteosclerosis (subchondral osteosclerosis DCS compared to Sham on week 1 and 2: p<0.001) - synovitis (week 2) - thickened synovial membrane (week 2) -
Zahoor, 2016 <sup>51</sup>	Garcia, 1986 <sup>53</sup>	Huebner, 2013 <sup>40</sup>	McCulloch, 2019 <sup>52</sup>	McCulloch, 2019 <sup>52</sup>	irregular cartilage surface (week 10) - osteophyte formation (50% after 10 weeks and 67% after 20 weeks) - purplish-white repair tissue filling the defect (week 20) - chondrocyte lost in full thickness (in 4 specimens at 20 weeks) - reduced safranin o-fast staining (since week 10) - fibrillation (week 20) - proteoglycan loss (week 20)
8	32	26	8	8	osteophyte formation (3 of 8 animals on week 1, all animals on week 2, osteophyte BV/VT: compared to sham group on week 2: p<0.01) - subchondral sclerosis (compared to Sham on week 1: p<0.001) - synovitis (week 2)
Male	Male	Female	Male	Male	osteophyte formation (6 of 8 animals on week 1, all animals on week 2, osteophyte number DCS compared to sham group on week 1: p<0.01, osteophyte BV/VT compared to sham group on week 2: p<0.001) - subchondral osteosclerosis (subchondral osteosclerosis DCS compared to Sham on week 1 and 2: p<0.001) - synovitis (week 2) - thickened synovial membrane (week 2) -
3 months old	2-3 months	12 months old	2.5 months	2.5 months	irregular cartilage surface (week 10) - osteophyte formation (50% after 10 weeks and 67% after 20 weeks) - purplish-white repair tissue filling the defect (week 20) - chondrocyte lost in full thickness (in 4 specimens at 20 weeks) - reduced safranin o-fast staining (since week 10) - fibrillation (week 20) - proteoglycan loss (week 20)
-	2500 - 3000 g	-	22-28 g	22-28 g	osteophyte formation (3 of 8 animals on week 1, all animals on week 2, osteophyte BV/VT: compared to sham group on week 2: p<0.01) - subchondral sclerosis (compared to Sham on week 1: p<0.001) - synovitis (week 2)
8 weeks	1,2,4,8,5, 12.5 weeks	3 days (n=6), 3 weeks (n=6), 6 weeks (n=6), 9 weeks (n=6), 52 weeks (n=2)	1,2,4 weeks	1,2,4 weeks	osteophyte formation (6 of 8 animals on week 1, all animals on week 2, osteophyte number DCS compared to sham group on week 1: p<0.01, osteophyte BV/VT compared to sham group on week 2: p<0.001) - subchondral osteosclerosis (subchondral osteosclerosis DCS compared to Sham on week 1 and 2: p<0.001) - synovitis (week 2) - thickened synovial membrane (week 2) -
-	2 weeks	-	1 (n=6), 2 (n=2)	1 (n=3),	irregular cartilage surface (week 10) - osteophyte formation (50% after 10 weeks and 67% after 20 weeks) - purplish-white repair tissue filling the defect (week 20) - chondrocyte lost in full thickness (in 4 specimens at 20 weeks) - reduced safranin o-fast staining (since week 10) - fibrillation (week 20) - proteoglycan loss (week 20)
Mankin score: (8.8 ± 1.4)	-	Mankin Score: week 10: (medial Femur: 7±2.14, lateral Femur: 3.80±1.30, medial Tibia: 7.78±2.44, lateral Tibia: 2.17±0.75) - week 20: (medial Femur: 11.13±2.10, lateral Femur: 8.75±2.92, medial Tibia: 9.40±1.84, lateral Tibia: 9.00±2.71)	-	-	osteophyte formation (3 of 8 animals on week 1, all animals on week 2, osteophyte BV/VT: compared to sham group on week 2: p<0.01) - subchondral sclerosis (compared to Sham on week 1: p<0.001) - synovitis (week 2)
irregular cartilage surface - reduced safranin o-fast staining - proteoglycan loss	irregular cartilage surface (week 1) - fibrosis (week 1) - osteophyte formation (week 2) - deep ulceration (week 4) - fibrillation (week 1 and 2) - synovial cell hypertrophy (week 1)	rough articular surface (since week 6) - cartilage loss (since week 6) - reduced safranin o-fast staining (since week 3) - fibrillation (week 3) - thickened synovial membrane (at week 9 and 52) - expression of MMP13 of the tibial plateau (significantly higher at 72 h and was not different from baseline values by 3w (p<0.025)) - expression of TGFβ of the tibial plateau (was significantly higher at 72 h and 3w (p<0.05)) - expression of IL-1β, IL-1Ra, IL-6, and IL-8 (was significantly increased at 72 h (p<0.01))	-	-	osteophyte formation (6 of 8 animals on week 1, all animals on week 2, osteophyte number DCS compared to sham group on week 1: p<0.01, osteophyte BV/VT compared to sham group on week 2: p<0.001) - subchondral osteosclerosis (subchondral osteosclerosis DCS compared to Sham on week 1 and 2: p<0.001) - synovitis (week 2) - thickened synovial membrane (week 2) -

a: the exact scoring system has been explained in the article, b: actually, DMM, b: surgery has been applied with 2 different methods: 30 mice by stereomicroscope and 30 mice by naked eye but results were the same, c: the details of procedure in each of these three articles were different.

Abbreviations: ACLT, Anterior cruciate ligament transection; OARS, Osteoarthritis Research Society International; MMP, Matrix metalloproteinase; MRI, Magnetic Resonance Imaging; CT, Computed tomography; ADAMTS, a disintegrin and metalloproteinase with a thrombospondin motifs; KOA, Knee osteoarthritis; DMM, Destabilization of medial meniscus; MMT, Medial meniscus transection; MMx, Medial meniscectomy; MCLT, Medial collateral ligament transection; PCLT, Posterior collateral ligament transection; LCLT, Lateral collateral ligament transection; PLT, Patellar ligament transection; pMM, partial Medial meniscectomy; MMPRT, Medial meniscus posterior root tear; OVx, Ovariectomy;

**Supplementary Table 2. Chemical models of knee osteoarthritis**

Intervention	Animal	Dosage	Saline volume (µL)	First author, year	Number of models	Sex	Age	Weight	Checkpoints after	Osteophyte	KOA score	KOA related changes				
MIA injection	New Zealand white rabbits	2.	2	V	1	M	7	∧	4	-	O	-				
												rough articular surface - cartilage loss - irregular cartilage surface - reduced alcian blue staining – matrix loss				
		3 mg MIA	2	G	3	-	-	-	3	1	-	O	irregular cartilage surface			
													irregular cartilage surface			
		4 mg	2	V	1	M	7	∧	∧	4	-	O	irregular cartilage surface - chondrocyte loss in full thickness - reduced safranin o-fast staining - fibrillation -			
													-			
		5	2	R	6	-	-	-	3	4	4	O	deep ulceration - osteophyte formation - irregular cartilage surface			
													rough articular surface - cartilage loss - irregular cartilage surface - reduced alcian blue staining -matrix loss			
		6	3	G	3	-	-	-	3	1	-	M	rough articular surface - cartilage loss - irregular cartilage surface - reduced alcian blue staining -matrix loss			
													deep ulceration - osteophyte formation - irregular cartilage surface - chondrocyte loss in in full thickness - reduced safranin o-fast staining - subchondral sclerosis - synovial cell hypertrophy			
		8	3	S	1	M	8	-	1	4	8	-	-	osteophyte formation (since week 8) - sclerosis - irregular cartilage surface - subchondral sclerosis – erosion		
														rough articular surface - cartilage loss - irregular cartilage surface - reduced alcian blue staining – matrix loss		
		10	200	Reb	6	-	-	-	3500	4	4	4	OA	deep ulceration - osteophyte formation - irregular cartilage surface - chondrocyte loss in full thickness - reduced safranin o-fast staining - subchondral sclerosis - synovial cell hypertrophy		
														rough articular surface - cartilage loss - irregular cartilage surface - reduced alcian blue staining – matrix loss		
		MIA injection	Wistar rats	0.	5	G	1	M	-	1	2	-	S	-		
														irregular cartilage surface (since week 4) – reduced safranin o-fast staining (since week 2) - thickened synovial membrane (since week 4) - synovium fibrosis (since week 4)		
				0.03	50	GUI	18	Mal	-	-	150	2.4	-	-	Scor	osteophyte formation (since week 4) - cartilage loss (since week 4) - irregular cartilage surface (since week 4) - reduced safranin o-fast staining (since week 2) - thickened synovial membrane (since week 4)
																irregular cartilage surface (since week 8) - reduced safranin o-fast staining (since week 4) – fibrillation (since week 4) - erosion (since week 12) – fissure (since week 8) - denudation of the articular cartilage (since week 12)
				0.1	50	GUI	18	Mal	-	-	150	2.4	4	-	-	osteophyte formation (since week 4) - cartilage loss (since week 4) - irregular cartilage surface (since week 4) - reduced safranin o-fast staining (since week 2) - thickened synovial membrane (since week 4)
																irregular cartilage surface (since week 8) - reduced safranin o-fast staining (since week 4) – fibrillation (since week 4) - erosion (since week 12) – fissure (since week 8) - denudation of the articular cartilage (since week 12)
0.2 mg	30			B	30.5	M	-	2.25	-	274.	3	-	-	osteophyte formation (since week 4) - irregular cartilage surface (since week 4) – proteoglycan loss (since week 4)		
														osteophyte formation (since week 2) - cartilage loss (since week 2) - irregular cartilage surface (since week 2) - reduced stain of safranin o-fast (since week 2) - subchondral sclerosis (since week 2) - thickened synovial membrane (since week 2)		
0.3 mg	50			GUING	18	Male	-	-	150 g	2.4	2 weeks	-	-	osteophyte formation (since week 2) - cartilage loss (since week 2) - irregular cartilage surface (since week 2) - reduced stain of safranin o-fast (since week 2) - subchondral sclerosis (since week 2) - thickened synovial membrane (since week 2)		
														-		
0.	5			Y	8	M	-	-	a	2	-	-	-	-		
														-		
1 mg MIA	30			Takahashi	30.5	Male	2.25	-	274.5 ±	3 days.	8 weeks	-	-	Knee Joint destruction (since week 8) - osteophyte formation (since week 8) - fibrosis (since week 8) - irregular cartilage surface (since week 4) - reduced safranin o-fast staining (since week 1) - fibrillation (since week 1) - erosion (since week 2) - fissure (since week 2) - denudation of the articular cartilage (since week 8)		
														irregular cartilage surface (week 2) - chondrocyte loss in in full thickness (week 2)		
1.5 mg	25			Oka	1	Mal	-	-	200–	2	-	-	-	deep ulceration (week 2) - irregular cartilage surface (week 2) - fibrillation (week 2) - infiltration of subchondral bone (week 2)		
														deep ulceration (since week 3) - osteophyte formation (on week 3 and 4) (two out of three animals at each checkpoint) - cartilage loss (since week 2) - irregular cartilage surface (since week 2) - chondrocyte loss in full thickness (since week 3) - fibrillation - subchondral thickening - proteoglycan loss - fissure - cloning of chondrocytes		
3	25			Fermiho	12	Male	-	-	280 ±	1,2,3,4	3 weeks	-	-	osteophyte formation (on week 2) - cartilage loss (on week 2) - irregular cartilage surface (on week 2) - reduced safranin o-fast staining (since week 2) - subchondral sclerosis (since week 2) - synovial membrane thickness (since		
														osteophyte formation (on week 2) - cartilage loss (on week 2) - irregular cartilage surface (on week 2) - reduced safranin o-fast staining (since week 2) - subchondral sclerosis (since week 2) - synovial membrane thickness (since		



SDF-1	Japanese white rabbits	3 times	-	Li.	9	-	3	2000 -	4,8,12	12	-	-	-	-	-	structure destruction (week 12) - osteophyte formation (week 12) - rough articular surface (week 8) - deep ulceration (week 8) - osteophyte formation (week 12) - cartilage loss (week 12) - irregular cartilage surface (week 8) - fissure (week 12)
		3 times	-	Li.	9	-	3	2000 -	4,8,12	12	-	-	-	-	-	structure destruction (week 12) - osteophyte formation (week 12) - rough articular surface (week 8) - deep ulceration (week 8) - osteophyte formation (week 12) - cartilage loss (week 12) - irregular cartilage surface (week 4) - chondrocyte loss in full thickness (week 12) - fissure (week 8)
H2O2	Wistar rats	H	-	K	2	5	M	2.	3	3	5	-	-	-	-	-
		H	-	K	2	5	M	2.	3	3	5	-	-	-	-	-
		H	-	K	2	5	M	2.	3	3	5	-	-	-	-	-
		H	-	K	2	5	M	2.	3	3	5	-	-	-	-	-
		H	-	K	2	5	M	2.	3	3	5	-	-	-	-	-
		H	-	K	2	5	M	2.	3	3	5	-	-	-	-	-
interlukin-1	New Zealand white rabbits	IL-	-	Bore	6	6	-	-	3000	1	-	-	-	-	-	irregular cartilage surface (3 out of 6 animals) - chondrocyte loss in full thickness (4 out of 6 animals) - Chondrocyte disorganization (5 out of 6 animals) - synovitis (6 out of 6 animals) - fissuring (5 out of 6 animals)
		IL-	-	Bore	9	9	-	-	3000	1	-	-	-	-	-	irregular cartilage surface (7 out of 9 animals) - chondrocyte loss in full thickness (6 out of 9 animals) - Chondrocyte disorganization (7 out of 9 animals) - synovitis (9 out of 9 animals) - fissure (2 out of 9 animals)
		I	-	B	4	4	-	-	3	1	-	-	-	-	-	synovitis (2 out of 4 animals)
		IL-	-	Bore	6	6	-	-	3000	1	-	-	-	-	-	irregular cartilage surface (4 out of 4 animals) - chondrocyte loss in full thickness (4 out of 4 animals) - chondrocyte disorganization (4 out of 4 animals) - synovitis (4 out of 4 animals) - fissure (4 out of 4 animals)
interlukin-17	New Zealand white rabbits	150 ng IL-17	1 ml each	Wang, 2017 <sup>20</sup>	15	-	-	approximate1	3 days and	6 weeks	-	-	-	-	-	Joint space narrowing (week 6) - osteophyte formation (week 6) - sclerosis (week 6) - mild deformity of subchondral bone (week 6) - rough articular surface (week 3) - cartilage loss (week 6) - irregular cartilage surface (week 6) - chondrocyte loss in in full thickness (week 6) - reduced safranin o-fast staining (1 week) - increased number of lacunae in subchondral bone (week 3) - cracking of the cartilage (week 6) - subchondral sclerosis (week 12) - thickened synovial membrane (week 3) - fissure (week 6)
		30 ng IL-17	1 ml each	Wang, 2017 <sup>20</sup>	15	-	-	approximate1	3 days and	6 weeks	-	-	-	-	-	Joint space narrowing (week 6) - osteophyte formation (week 6) - sclerosis (week 6) - mild deformity of subchondral bone (week 6) - rough articular surface (week 3) - cartilage loss (week 6) - irregular cartilage surface (week 6) - chondrocyte loss in in full thickness (week 6) - reduced safranin o-fast staining (week 1) - increased number of lacunae in subchondral bone (week 3) - cracking of the cartilage (week 6) - subchondral sclerosis (week 12) - thickened synovial membrane (week 3) - fissure (week 6)
		3 ng	1 ml	Wan	15	-	-	appr	3	12	-	-	-	-	-	Joint space narrowing (week 12) - osteophyte formation (low level at week 12) - reduced safranin o-fast staining (week 1) - thickened synovial membrane (week 12)
New Zealand white	4% papain	-	-	Li, 2016 <sup>71</sup>	6	Male and	-	approxima	6 weeks	-	-	-	-	-	-	fibrosis changes - rough articular surface - ulceration - osteophyte formation - irregular cartilage surface - chondrocyte lost in full thickness - reduced safranin o-fast staining - reduced number of cytoplasmic organelles - swelling mitochondria, lipid droplets, vacuoles and glycogen particle aggregation in the cytoplasm - loose collagen network - nuclei became irregular and nuclear pyknosis appeared serrated
		-	-	Li, 2016 <sup>71</sup>	6	Male and	-	approxima	3 weeks	-	-	-	-	-	-	fibrosis - rough articular surface - ulceration - osteophyte formation - irregular cartilage surface - chondrocyte lost in full thickness - reduced safranin o-fast staining - reduced number of cytoplasmic organelles - swelling mitochondria, lipid droplets, vacuoles and glycogen particle aggregation in the cytoplasm - loose collagen network - nuclei became irregular and nuclear pyknosis appeared serrated
		-	-	Li, 2016 <sup>71</sup>	6	Male and	-	approxima	6 weeks	-	-	-	-	-	-	fibrosis - rough articular surface - ulceration - osteophyte formation - irregular cartilage surface - chondrocyte lost in full thickness - reduced safranin o-fast staining - reduced number of cytoplasmic organelles - swelling mitochondria, lipid droplets, vacuoles and glycogen particle aggregation in the cytoplasm - loose collagen network - nuclei became irregular and nuclear pyknosis appeared serrated
		-	-	Li, 2016 <sup>71</sup>	6	Male and	-	approxima	3 weeks	-	-	-	-	-	-	fibrosis - rough articular surface - ulceration - osteophyte formation - irregular cartilage surface - chondrocyte lost in full thickness - reduced safranin o-fast staining - reduced number of cytoplasmic organelles - swelling mitochondria, lipid droplets, vacuoles and glycogen particle aggregation in the cytoplasm - loose collagen network - nuclei became irregular and nuclear pyknosis appeared serrated
guinea pig	Papain	-	-	Kopp,	6	Male	12	820-	8,16,24,	1	-	-	-	-	-	irregular cartilage surface (since hour 6 - subchondral sclerosis (since week 32) - erosion (since week 32)
		-	-	Kopp,	6	Male	12	820-	8,16,24,	1	-	-	-	-	-	Knee joint structure destruction (week 32) - sclerosis (week 32) - irregular cartilage surface (since week 8) - chondrocyte lost in full thickness (week 40)- reduced alcian blue staining (week 40) - fibrillation (since week 24) - subchondral sclerosis (since week 24) - erosion (since week 32)
6-ml	-	Van	2.5	Mal	2.5	-	-	-	-	-	-	-	-	-	-	fibrillation (day 1) - thickened synovial membrane (day 3) - erosion of noncalcified cartilage (day 1)

Abbreviations: MIA, Monoiodoacetate; OARS, Osteoarthritis Research Society International; KOA, Knee osteoarthritis

Supplementary Table 3. Mechanical models of knee osteoarthritis

Intervention	Animal	Exact intervention	First author,	Number of models	Sex	Age	Weight	Checkpoints	Osteophyte	KOA score	KOA related findings
Loading C57Bl/6 mice		subjected the left tibiae to cyclic compressive loading at a 9.0 N peak load	Ko, 2013 <sup>90</sup>	21	Male	2.5 months old	-	1, 2, 6 weeks	week 6	-	reduced safranin o-fast staining - cartilage fibrillation - cartilage fragmentation - cartilage erosion - cartilage thinning - decrease of the epiphyseal bone mass - increased trabecular separation - the metaphyseal bone mass increased by 20% - trabecular thickening increased by 32% - thickening of the subchondral cortical bone at the posterior-lateral aspect of the tibial plateau - osteophyte formation (week 6)
		subjected the left tibiae to cyclic compressive loading at a 4.5 N peak load	Ko, 2013 <sup>90</sup>	21	Male	6.5 months	-	1, 2, 6 weeks	-	-	reduced safranin o-fast staining - slight cartilage surface fibrillation - thickening of the subchondral cortical bone at the posterior-lateral aspect of the tibial plateau
		subjected the left tibiae to cyclic compressive loading at a 9 N peak load	Ko, 2103 <sup>90</sup>	21	Male	6.5 months old	-	1, 2, 6 weeks	week 6	-	reduced safranin o-fast staining - cartilage fibrillation - cartilage fragmentation - cartilage erosion - cartilage thinning - almost full thickness cartilage loss (week 6) - decrease of the epiphyseal bone mass - decreased numbers of trabeculae - thickening of the subchondral cortical bone at the posterior-lateral aspect of the tibial plateau - osteophyte formation (week 6)
		axial compressive loads were applied through the knee joint (peak force of 3 N). At the start of the loading session, a 0.5 N compressive preload was applied. then Sixty cycles of loading were applied. Each cycle consisted of a triangle wave with a rise time to peak force of 0.17 s and a fall time of 0.17 s followed by a 10 s rest period (holding at 0.5 N)	Wu, 2014 <sup>89</sup>	13	Male	2 months old	-	5,9 days and 2 weeks	-	-	reduced safranin o-fast staining - chondrocyte apoptosis - fibrillation - cartilage matrix degradation - disruption of cartilage collagen fibril arrangement
		axial compressive loads were applied through the knee joint (peak force of 6 N). At the start of the loading session, a 0.5 N compressive preload was applied. Sixty cycles of loading were then applied. Each cycle consisted of a triangle wave with a rise time to peak force of 0.17 s and a fall time of 0.17 s followed by a 10 s rest period (holding at 0.5 N)	Wu, 2014 <sup>89</sup>	13	Male	2 months old	-	5,9 days and 2 weeks	-	-	reduced safranin o-fast staining - synovitis (day 5) - chondrocyte apoptosis - fibrillation - cartilage matrix degradation - disruption of cartilage collagen fibril arrangement
		axial compressive loads were applied through the knee joint (peak force of 9 N). At the start of the loading session, a 0.5 N compressive preload was applied. Sixty cycles of loading were then applied. Each cycle consisted of a triangle wave with a rise time to peak force of 0.17 s and a fall time of 0.17 s followed by a 10 s rest period (holding at 0.5 N)	Wu, 2014 <sup>89</sup>	13	Male	2 months old	-	5,9 days and 2 weeks	-	-	tearing of the anterior cruciate ligament - reduced safranin o-fast staining - synovitis (day 5) - chondrocyte apoptosis - fibrillation - cartilage matrix degradation - disruption of cartilage collagen fibril arrangement - localized decrease in cell density and increase in proteoglycan-rich matrix staining (day 9) - localized type II collagen costaining with aggrecan (week 2)

	9 N axial compressive loads were applied for forty cycles with six loading episodes over a period of 2 weeks	ramos-mucci,	-	Male	2.5 months old	-	-	-	increased knee joint space mineralization (week 4 and 14) - Increases of red collagen birefringence in the posttrauma ACL-tibial enthesis - collagen type II expanded to mid-substance region - expression of chondrogenic marker SOX9, hypertrophic marker RUNX2 and small-leucine rich proteoglycan ASPN	
	Loading force of 55 N at a rate of 20 N/sec with the indenter displacement limit of -2 to -6 mm to the tibial plateau	Stiffel, 2021 <sup>84</sup>	24	Male and female	3 months old	-	5, 11 weeks	week 5	Mankin score: (average) cartilage erosion (week 5) -irregular subchondral bone (week 5) - calcified cartilage (week 5) - reduced safranin o-fast staining (weeks 5) - osteophyte formation (week 5) - loss of articular cartilage (week 5) disorganization of chondrocytes (week 5) - meniscal hyperplasia and mineralization (week 5)	
	2.0 mm of tibial displacement to incite a full rupture of ACL	Timkovich,	30	Male and	3 months old	-	1, 3 days and	-	OARSI	
	The load was applied in spike form over a 50 ms interval at 60 cycles/min for 40 min, 5 days/week the loading was maintained within 10% of 1.5 times body weight virtually the entire daily treatment period.	Radin, 1984 <sup>97</sup>	33	Female	-	3500 - 4500	1, 2, 3 days	-	-	cartilage fibrillation (75% of the rabbits after 3 weeks) - complete splitting of the cartilage matrix from the superficial to the deep layers (week 3 and 6) - deposition of calcium (week 3) - increase of intracartilaginous cysts (week 6)
	The spring-loaded device delivered reproducible impacts with the following characteristics: Impact area (mm <sup>2</sup> )=1.39 ± 0.11, Time to peak (ms)=0.32 ± 0.04, Peak force (N)=236 ± 95.2, Normalized peak impact stress (MPa)= 169 ± 68.4, Maximum displacement (%)=21.5 ± 4.5, Spring potential energy (J)=0.27783 - Loading rate to peak force (×10 <sup>3</sup> N/s)=737.5 ± 182, Average stress rate (×10 <sup>3</sup> MPa/s)=528.1 ± 69, Average strain rate(×10 <sup>3</sup> %/s)=67.2 ± 4.6	Alexander, 2012 <sup>115</sup>	30	Female	18 - 24 months old	-	1 day, 4, 12 weeks	-	-	reduced safranin o-fast staining (1 day) - proteoglycan loss (week 12) - cell loss (week 12) - deep fissuring (week 12) - clonal expansion (week 12)
New Zealand white rabbits	knees were loaded using submaximal (concentric (n=8), isometric(n=7) or eccentric(n=8)) stimulation of the quadriceps muscles three times a week for 28 days (=13 stimulation sessions) by means of a femoral nerve cuff. The duration for each exercise trial was 50 min with repeat cycles of 500 ms of stimulation followed by a 1500 ms break. If muscles fatigued, short breaks were added every 200 stimulation cycles.	Horisberger, 2013 <sup>97</sup>	23	Male	12 months old	-	1 day after the last exercise	-	-	significantly higher cell death rates than the control joints (The isometric group animals showed significantly more cell death than the concentric group animals) - Cell density was significantly decreased compared to control joints in the lowest third of the cartilage
CBA mice	were loaded on alternate days, 3 times each week for 2 weeks. each time a single loading pattern in which peak loads of 9 N were applied for 0.05 seconds, with a rise and fall time each of 0.025 seconds and a baseline hold time of 9.9 seconds. Baseline 2 N loads maintained the tibia in position between periods of peak loading. Forty cycles of this pattern were applied to the right knee in each loading episode.	Poulet, 2011 <sup>96</sup>	14 (each timepoint n=7)	Male	2 months old	-	2 days, 3 weeks after	2 days after the final	-	reduced safranin o-fast staining (since day 2) - Chondrocyte clustering (since day 2) - chondroplasia (since day 2) - joint space narrowing (since day 2) - osteophyte formation (since day 2) - proteoglycan loss (since day 2) - synovium fibrosis (since day 2)

Sprague-Dawley rats	<p>were loaded 3 times each week for 5 weeks. each time a single loading pattern in which peak loads of 9 N were applied for 0.05 seconds, with a rise and fall time each of 0.025 seconds and a baseline hold time of 9.9 seconds. Baseline 2 N loads maintained the tibia in position between periods of peak loading. Forty cycles of this pattern were applied to the right knee in each loading episode.</p>	Poulet, 2011 <sup>96</sup>	9	Male	2 months old	-	2 days after final loading	2 days after the final	reduced safranin o-fast staining - Chondrocyte clustering - chondroplasia - joint space narrowing - osteophyte formation - proteoglycan loss - synovium fibrosis
	<p>were loaded for a single episode in which peak loads of 9 N were applied for 0.05 seconds, with a rise and fall time each of 0.025 seconds and a baseline hold time of 9.9 seconds. Baseline 2 N loads maintained the tibia in position between periods of peak loading. Forty cycles of this pattern were applied to the right knee in each loading episode.</p>	Poulet, 2011 <sup>96</sup>	12 (each timepoint n=6)	Male	2 months old	-	2 hours, 2 weeks	week 2	joint space narrowing (since 2 hours) - proteoglycan loss (since 2 hours) - chondroplasia (week 2) - osteophyte formation (week 2)
	<p>axial compressive loading 3 times per week for 5 weeks (The loading pattern consisted of a trapezoidal wave, with peak 9 N loads for 0.05 s, rise and fall times 0.025 s each and baseline hold time of 9.9 s at 2 N. Forty cycles were applied in each loading episode.)</p>	Poulet, 2015 <sup>100</sup>	5	Male	2 months old	-	2 days after final	-	increased subchondral bone thickening - increased trabecular thickness - increased BV/TV (Bone volume over total volume)
	<p>One impact load of 53 N at a speed of 15 mm/s with a peak load maintained for 0.05 s was applied to the medial condyle of the right knee region at the periosteum-synovium junction in line with the medial collateral ligament (after a surgical procedure to expose the medial femoral condyle.)</p>	Venne, 2020 <sup>14</sup>	17	-	10 - 12 months old	-	1 day, 3, 6, 9 weeks	-	fibrosis (week 3) - hypertrophic chondrocyte (week 3) - dense cambium periosteum layer (week 3) - more collagen rich in the synovial membrane (week 9) - projection of bone tissue formation (week 9)
	<p>All animals underwent surgery to attach transcutaneous bone plates to the lateral aspect of the left tibia and femur. Following a 2-week recovery, rats were fit with a VLD and the spring torque set to apply compressive load alteration (100% body weight) in addition to the normal compressive forces in the joint produced by muscle forces and ambulation. The VLD was engaged 24 h per day.</p>	Roemhildt, 2013 <sup>98</sup>	5	Male	9 months old	666 ± 32 g	6 weeks after start of	-	proteoglycan loss - loss of chondrocytes - fibrillation - periarticular fibrosis - lower Articular cartilage aggregate modulus (medial compartment) - increased surface matrix loss width - increased Degenerated cartilage area - increased Significant cartilage degeneration width (medial compartment) - decreased mean cellularity (medial compartment)
	<p>All animals underwent surgery to attach transcutaneous bone plates to the lateral aspect of the left tibia and femur. Following a 2-week recovery, rats were fit with a VLD and the spring torque set to apply compressive load alteration (100% body weight) in addition to the normal compressive forces in the joint produced by muscle forces and ambulation. The VLD was engaged 24 h per day.</p>	Roemhildt, 2013 <sup>98</sup>	6	Male	9 months old	666 ± 32 g	20 weeks after start of loading	-	loss of chondrocytes - increased matrix fibrillation and erosion - peripheral chondrophyte/osteophyte - fibrillation - periarticular fibrosis - lower Articular cartilage aggregate modulus (medial compartment) - decreased articular cartilage thickness (medial compartment) - increased subchondral bone thickness (medial compartment) - increased calcified cartilage thickness (lateral compartment) - increased surface matrix loss width - increased Degenerated cartilage area - increased Significant cartilage degeneration width (medial compartment) - decreased mean cellularity (medial compartment)

Wistar rats	a single compression session, which included 60 cycles of cyclic loading, One cycle included a preload of 5 N and a peak load of 20 N, with an approaching speed of 1 mm/s following 10-s rest intervals.	Zhao, 2022 <sup>94</sup>	36 (n=6 at each timepoint)	Male	3 months old	-	1, 2, 4, 8, 24, 48	-	-	cartilage damage - chondrocytes decrease - mild synovitis (week 4) - cell clustering and cyst formation (week 24) - cleft formation (week 48) - high expression of MMP13
	in vivo 60 cycles of 20 N dynamic compression on the knee articular cartilage	Ji, 2021 <sup>101</sup>	20	Male	3 months old	-	3 days, 1, 2,	-	-	smaller cartilage lesion area volume - faster recovery of superficial lubricin - focal type II collagen over expression in the articular cartilage lesion
	in vivo 60 cycles of 50 N dynamic compression on the knee articular cartilage	Ji, 2021 <sup>101</sup>	20	Male	3 months old	-	3 days, 1, 2,	-	-	larger cartilage lesion area volume - longer recovery of superficial lubricin - focal type II collagen over expression in the articular cartilage lesion
Lewis rats	a static preload of approximately 5.4 N was applied for 15–25 s followed by a single $3.26 \pm 0.28$ N/s ramp in compressive load until the ACL rupture was observed. (70% of ruptures occurred during the first compressive load (n = 19), In the other animals, rupture was achieved after a second (n = 5) or third (n = 3) compressive load)	Brown, 2020 <sup>86</sup>	24 (n=6 at each timepoint)	Male	3.2 - 3.6 months old	$356.2 \pm 16.9$ g	4, 8, 12, 16 weeks	week 16	-	ossification of the anterior menisci and bone remodeling (since week 4) - Macroscopic bone erosion (since week 8) - osteophyte (in the medial tibia by 16 weeks) - increased subchondral bone porosity (just at week 4) - proteoglycan loss in the femoral cartilage and cartilage swelling in the anterior femur (since week 4) - cartilage fibrillation and lamination (since week 8) - cartilage erosion to the tidemark in the anterior femur and posterior tibia (week 12) - chondrocyte hypertrophy (since week 4) - Chondrocyte clustering (since week 4 until week 16 but only significantly greater at week 4) - Tidemark duplication (in the anterior tibial cartilage at week 16) - synovitis (since week 4) - higher IL-6, IL-1 $\beta$ (highest at week 8), TNF- $\alpha$ (highest at week 8) and collagen type II breakdown in injured animals compared to control animals
Str./ort mice	Forty cycles were applied, 3 times/week for 2 weeks. in each cycle Compression was applied through the knee with 9 N peak for 0.05 s, rise and fall-time of 0.025 s and 9.9 s baseline holdtime. Baseline 2 N loads maintained tibiae in place between loading episodes.	Poulet, 2013 <sup>91</sup>	8	Male	2 months old	-	2 days after final	-	-	reduced safranin o-fast staining - proteoglycan loss - reduction of Collagen type II - synovial intimal layer hyperplasia (4 out of 8 animals) - cruciate ligament cell hypertrophy (6 out of 8 animals) - cruciate ligament greater matrix staining intensity (6 out of 8 animals) - cruciate ligament cell clusters (4 out of 8 animals)
Immobilization rabbits	periodic immobilization: (4(Number of immobilization periods)-7(Length of immobilization period in days)-7(Length of the period between each immobilization in days))	Videman, 1982 <sup>99</sup>	18	-	9 months old	-	at the end of	-	-	mean osteoarthritic changes found in radiographs: slight OA at each checkpoint but worsens over time - thickening of the joint capsule and the collateral ligaments - Fibrillation - irregular proliferation - variation in thickness and regional disappearance of articular cartilage - subcondral cysts and sclerosis

periodic immobilization: (5(Number of immobilization periods)-7(Length of immobilization period in days)-28(Length of the period between each immobilization in days))	Videman, 1982 <sup>99</sup>	16	-	9 months old	-	at the end of	week 22	mean osteoarthritic changes found in radiographs: slight OA at the end of immobilization and moderate OA after 22 weeks - after 22 weeks: (thickening of the joint capsule and the collateral ligaments - Fibrillation - irregular proliferation - variation in thickness and regional disappearance of articular cartilage - subcortical cysts and sclerosis - Osteophyte formation)
periodic immobilization: (4(Number of immobilization periods)-10(Length of immobilization period in days)-4(Length of the period between each immobilization in days))	Videman, 1982 <sup>99</sup>	12	-	9 months old	-	at the end of immobilization,	week 32	mean osteoarthritic changes found in radiographs: slight OA at the end of immobilization and after 8 weeks (worsens over time) , moderate OA after 32 weeks - after 32 weeks: (thickening of the joint capsule and the collateral ligaments - Fibrillation - irregular proliferation - variation in thickness and regional disappearance of articular cartilage - subcortical cysts and sclerosis - Osteophyte formation)
periodic immobilization: (12(Number of immobilization periods)-4(Length of immobilization period in days)-10(Length of the period between each immobilization in days))	Videman, 1982 <sup>99</sup>	12	-	9 months old	-	at the end of	week 22	mean osteoarthritic changes found in radiographs: slight OA at the end of immobilization and moderate OA after 8 weeks and 22 weeks (worsens over time) - after 22 weeks: (thickening of the joint capsule and the collateral ligaments - Fibrillation - irregular proliferation - variation in thickness and regional disappearance of articular cartilage - subcortical cysts and sclerosis - Osteophyte formation)
35 days of Continuous immobilization	Videman,	12	-	9 months old	-	at the end of	-	mean osteoarthritic changes found in radiographs: slight OA after 8 weeks
49 days of Continuous immobilization	Videman,	9	-	9 months old	-	at the end of	-	mean osteoarthritic changes found in radiographs: slight OA at the end of immobilization and moderate OA after 8 weeks
immobilization periods varying from 4 days to 14 days with elastic splint	Langenskiöld,	44	-	-	-	4 days - 2 weeks	week 2	increase of uptake of 35S-sulphate in the ligaments (day 4) - abnormally proliferating cartilage in peripheral to the edges of the joint both on the femur and the tibia (day 10) - osteophyte formation (week 2) - thickening of the periarticular soft tissue (week 1)
immobilization periods varying from 15 days to 28 days with elastic splint	Langenskiöld	41	-	-	-	2-4 weeks	week 3	fibrillation (week 3) - loss of cartilage (week 3) - erosion and necrosis of articular cartilage (week 3) - fissure (week 3) - osteophyte formation (week 3) - thickening of the distal end of the femur (week 3)

	immobilization periods varying from 29 days to 80 days with elastic splint	Langenskiöld	96	-	-	-	4 - 11.5	week 6	Loss of articular cartilage (more than other groups) - thickening of the distal end of the femur (week 6) - osteophyte formation (week 6) - area of denuded bone (week 6)
	immobilization periods varying from more than 80 days with elastic splint	Langenskiöld	50	-	-	-	more than	-	eburnation of denuded bone - areas of hypertrophied cartilage
Running wistar rats	Intracranial Self-Stimulation (ICSS) resulting in running a total distance of 30 km within a period of 12 weeks. (500 m/day for a 5 day/week)	Pap, 1998 <sup>92</sup>	10	Male	3.25 - 3.5 months old	250 - 300 g	12 weeks	-	fibrillations - clefts in joint cartilage - cell cloning - moderate or severe reduced safranin o-fast staining - an increasing number of MMP-3 immunoreactive chondrocytes (an average of 89.9% of all visible chondrocytes showed immunoreactivity to MMP-3 (control=47%))
	Intracranial Self-Stimulation (ICSS) resulting in running a total distance of 15 km within a period of 6 weeks. (500 m/day for a 5 day/week)	Pap, 1998 <sup>92</sup>	10	Male	3.25 - 3.5 months old	250 - 300 g	6 weeks	-	irregular cartilage surface - cell cloning - slight reduced safranin o-fast staining - an increasing number of MMP-3 immunoreactive chondrocytes (an average of 70.4% of all visible chondrocytes showed immunoreactivity to MMP-3 (control=47%))
	the rats ran 1 km in 55 min, twice a day (6 h apart), 5 days per week resulting in a total distance of 30 km in 3 weeks	Beckett, 2012 <sup>95</sup>	3	Male	4 - 4.5 months old	471 ± 50 g	3 weeks	-	irregular cartilage surface - proteoglycan loss - generally reduction of Collagen type II - Spotty increases of MMP-13 in the cartilage matrix - the proportion of the calcified cartilage zone in full thickness of articular cartilage was increased 60%(p<0.05)
	the rats ran 1 km in 55 min, twice a day (6 h apart), 5 days per week resulting in a total distance of 55 km in 6 weeks	Beckett, 2012 <sup>95</sup>	3	Male	4 - 4.5 months old	471 ± 50 g	6 weeks	-	irregular cartilage surface - proteoglycan loss - formation of large cysts - chondrocyte clusters Around the cysts - generally reduction of Collagen type II (spotty areas around cartilage lesions had increased type II collagen deposition) - unevenly distribution of Type II collagen and proteoglycan in the cartilage matrix - Spotty increases of MMP-13 in the cartilage matrix - the proportion of the calcified cartilage zone in full thickness of articular cartilage was increased 80% (p < 0.001)
Abbreviations: OARSI, Osteoarthritis Research Society International; OA, osteoarthritis; KOA, Knee osteoarthritis; MMP, Matrix metalloproteinase.									

**Supplementary Table 4. Genetic models of knee osteoarthritis**

Animal	Intervention	First author, year	Number of models	Age	Weight	Checkpoints after intervention	Osteophyte formation	KOA score	KOA related findings
C57BL/6 mice	Deletion of P58IPK	Gilbert , 2014 <sup>23</sup>	9	-	-	48-52 weeks, 92-100 weeks	48-52 weeks	-	osteophyte formation (48-52 weeks old) - narrower tibiae and shorter epiphyses in tibiae (in both 48-52 and 92-100 weeks old) - cartilage loss (48-52 weeks old) - irregular cartilage surface (48-52 weeks old) - chondrocyte lost (48-52 weeks old)
	Dot11 gene knockout	Cornelis, 2019 <sup>81</sup>	3	From birth	-	48,56 weeks	56 weeks	-	osteophyte formation (week 56) - Chondrocyte hypertrophy (week 56)
	heterozygous of gene Dot11 CART-KO	Cornelis, 2019 <sup>81</sup>	3	From birth	-	64 weeks	64 weeks	-	osteophyte formation - chondrocyte hypertrophy
	mutation of Clock gene + EntransterT M nanoparticles every 3 days over the course of 2 weeks	Yuan, 2019 <sup>80</sup>	30	From birth	-	24 weeks	-	-	irregular cartilage surface (week 24) - reduced safranin o-fast staining (week 24) - proteoglycan loss (week 24) - cartilage erosion (week 24) - significant increased expression of IL-6 (week 24)
crossing C57BL/6- <i>EFNB2</i> <sup>fl/fl</sup> with C57BL/6 <i>Col2-Cre</i> transgenic	deletion of ephrin-B2 ( <i>EFNB2</i> <i>Col2</i> KO)	Valverde-Franco , 2016 <sup>83</sup>	8	From birth	-	At birth – 2, 3,8,48 weeks	-	-	increased type X collagen (birth) - disorganized hypertrophic zone (birth) - decreased mineralization (birth) - significant reduction in VEGF (week 2) and TRAP (week 2) at the chondro-osseous junction - delay in the secondary ossification (week 2) - including a decrease in bone volume (week 2) - trabecular thickness (week 2) - reduced bone mineral density (week 2)
crossing C57BL/6- <i>Alk5</i> <sup>flox/flox</sup> with C57BL/6- <i>Col2a1-CreERT2</i> mice	deletion of <i>Alk5</i> gene	Wang, 2017 <sup>82</sup>	4	From birth	-	8,12,24 weeks	24 weeks	-	loss of proteoglycan (week 12) - increased number of hypertrophic chondrocytes (week 12) - severe loss of articular cartilage (week 24) associated with greater loss of proteoglycan (week 24) - osteophyte formation (week 24)
C57BL/6-SJL mice	overexpression of <i>Smurf2</i>	Wu, 2008 <sup>79</sup>	6	From birth	-	8,16,20,24,32,40 weeks	32 weeks	-	osteophyte formation (week 32) - increased mineralization of the meniscus (week 32) - chondrocyte proliferation (week 18) - reduced safranin o-fast staining - fibrillation (week 18) - increased expression of MMP-13 and type X collagen mRNA (week 24)
crossing C57BL/6J males with DBA/2J females	mutation in <i>Gdf5</i> (heterozygote)	Masuya, 2007 <sup>78</sup>	51	From birth	-	8,25 weeks	-	-	chondrocyte loss (week 8) - reduced safranin o-fast staining (week 8) - chondrocyte hypertrophy (week 8) - ankylosis (week 8)- fusing of the joint (week 8)
	mutation in <i>Gdf5</i> (homozygote)	Masuya, 2007 <sup>78</sup>	20	From birth	-	8,25 weeks	-	-	chondrocyte loss (week 8) - reduced safranin o-fast staining (week 8) - chondrocyte hypertrophy (week 8) - ankylosis (week 8)- fusing of the joints (week 8)
C57BL/6J <i>OlaHsd</i>	heterozygous knockout of <i>Col2a1</i> gene	Lapveteläinen ,	15	-	39.5±1.3 g	12,24,36,48,60 weeks	-	-	fibrillation - cell loss from the superficial zone - striation of the cartilage - deeper defects extending in the intermediate and deep zones of uncalcified cartilage - defects extending in the calcified cartilage - lesions

		2001 <sup>77</sup>							extending in the subchondral bone
	homozygous knockout of Col11a2 gene	Lapvet eläinen . 2001 <sup>77</sup>	15	2.5 months old	37.4±1.6 g	36, 60 weeks	-	-	fibrillation - cell loss from the superficial zone - striation of the cartilage - deeper defects extending in the intermediate and deep zones of uncalcified cartilage - defects extending in the calcified cartilage - lesions extending in the subchondral bone
Pip5k1cfl/fl mice crossing with the Aggrecan CreERT2 knock-in transgenic mice	deletion of Pip5k1c in aggrecan-expressing chondrocytes	Qu, 2023 <sup>74</sup>	6	From birth	-	20, 60 weeks	at 60 weeks old	-	osteophyte formation (60 weeks old) - sclerosis (60 weeks old) - irregular cartilage surface (60 weeks old) - chondrocyte lost (60 weeks old) - reduced safranin o-fast staining (60 weeks old) - chondrocyte apoptosis (60 weeks old) - subchondral sclerosis (60 weeks old) - chondrocyte hypertrophy (60 weeks old) - cartilage erosion (60 weeks old) - decrease of matrix fraction (60 weeks old) - surface fissures (60 weeks old) - meniscus deformation (60 weeks old) - synovial hyperplasia (60 weeks old)
agouti mouse	Overexpression of MIG-6	Bellini . 2020 <sup>73</sup>	12	From birth	-	24,44,48, 72 weeks	-	-	cartilage loss (48 weeks old) - irregular cartilage surface (48 weeks old) - cartilage erosion (48 weeks old) - proteoglycan loss (72 weeks old) - increased expression of MMP-13 (in both 48 and 72 weeks old)
Wistar rats	deletion mutation in the C-propeptide encoding region of Col2a1	Bomsta, 2006 <sup>76</sup>	5	From birth	-	12,24,36, 48,60,88 weeks	-	-	Decrease of matrix fraction (12 weeks old) - thinner cartilage (since 12 weeks old) - increased cell density (since 12 weeks old)
crossing Atg5-floxed mice with Col2-Cre mice	deletion of Atg5 in chondrocytes	Bouderlique, 2016 <sup>22</sup>	17	From birth	-	8,24,48 weeks	-	-	chondrocyte loss (8 weeks old) - Fibrillation (24 weeks old) - cartilage erosion (48 weeks old) - increased expression of MMP-13 (48 weeks old)
Mice	MIG-6 gene deletion	Zhang, 2005 <sup>72</sup>	-	From birth	-	4,6,8,12,16,20,22,24 weeks	12 weeks	-	abnormal gait as early as 4 weeks old - progressive enlargement and deformity of multiple joints (4 weeks) - outgrowths of abnormal bony nodules within the joint space adjacent to the margin of the synovial and cartilage junctions (6 weeks) - the inner zones have a higher density of proteoglycan produced by mature chondrocytes - Subchondral cyst formation (12 weeks) - Synovial hyperplasia (8 weeks) - proteoglycan loss (12 weeks) - osteophyte formation (12 weeks) - ankylosis and death (24 weeks)
Abbreviations: OARSI, Osteoarthritis Research Society International; KOA, Knee osteoarthritis; MMP, Matrix metalloproteinase.									

Supplementary Table 5. Hybrid models of knee osteoarthritis

Intervention	Animal	Exact intervention	First author, year	Number of models	Sex	Age	Weight	Checkpoints after intervention	Osteophyte formation	KOA score	KOA related findings
ACLT + MIA	New Zealand white rabbits	3 mg MIA injection 2 weeks after ACLT	Go, 2022 <sup>10</sup>	3	-	-	3500 ± 500 g	6 weeks	6 weeks	Modified Mankin score: femur: (7.89 ± 0.84), tibia: (3.33 ± 0.0)	rough articular surface - osteophyte formation (medial edge of the tibia) - cartilage loss - irregular cartilage surface - reduced alcian blue staining - matrix degeneration - calcified cartilage - reduction of Collagen type II - Tibial chondrocytes were disordered and had lost their lacuna

		6 mg MIA injection 2 weeks after ACLT	Go, 2022 <sup>10</sup>	3	-	-	3500 ± 500 g	6 weeks	6 weeks	Modified Mankin score: femur: (13.78 ± 0.19), tibia: (11.67 ± 0.33)	rough articular surface - deep ulceration - osteophyte formation (medial edge of the tibia and medial and lateral sides of the femur) - cartilage loss - irregular cartilage surface - reduced alcian blue staining - fibrillation - matrix degeneration - cartilage erosion - reduction of Collagen type II - loss of hematoxylin- eosin staining in most of the femoral cartilage
		9 mg MIA injection 2 weeks after ACLT	Go, 2022 <sup>10</sup>	3	-	-	3500 ± 500 g	6 weeks	6 weeks	Modified Mankin score: femur: (13.11 ± 0.38), tibia: (11.56 ± 0.38)	rough articular surface - deep ulceration - osteophyte formation (all over the rim of the outer femur and tibia) - cartilage loss - irregular cartilage surface - reduced alcian blue staining - fibrillation - matrix degeneration - calcified cartilage - cartilage erosion - reduction of Collagen type II - no chondrocytes were observed in the femur
ACLT + papain	New Zealand white rabbits	Injection of 4% papain and its activator 0.03 M L- cysteine in the first, fourth and seventh days in the right knee + ACLT three weeks after the last injection	Li, 2016 <sup>71</sup>	6	M & F	-	approxi mately 2500 – 3000 g	6 weeks after the last injection	6 weeks after the last injection	-	osteophyte formation - rough articular surface - deep ulceration - cartilage loss - irregular cartilage surface - chondrocyte loss in full thickness - reduced safranin o-fast staining - joint instability - broken and messy collagen texture - many denatured and necrotic chondrocytes - large lipid droplets - a lot of vacuoles - swelling of mitochondria
ACLT + pmm + Running	Sprague-Dawley rats	ACLT and pMM + forced mobilization beginning 5 days before surgery to train the animals. Each animal completed a 30 min session of mobilization on Mondays, Wednesdays and Fridays each week until being sacrificed	Applet on, 2007 <sup>37</sup>	24	M	-	300 - 325 g	2, 4, 8, 12, 16, 20 weeks after surgery (n=4 at each checkpo int)	20 weeks	OARSI scoring system: week 20: (22.375± 0.718)	osteophyte formation (week 20) - loss of subchondral trabecular architecture (week 12) - cartilage fibrosis (week 4) - rough articular surface (week 4) - abraded joint surface (week 4) - irregular cartilage surface (week 2) - reduced safranin o-fast staining (week 2) - chondrocyte clusters (week 4) - subchondral sclerosis (week 12) - chondrocyte hypertrophy - Matrix erosion (week 8) - infiltration of bone marrow stromal cells (week 2) - proteoglycan loss (week 2) - cartilage delamination (week 2) - cartilage fissuring (week 2) - presence of Collagen type X (since week 8) - reduction of Collagen type II (week 4) - increased expression of MMP13 (since week 4) - increased alkaline phosphatase expression (week 8 and 12)
Running + H2O2	Wistar rats	H2O2(2% ,0.05 ml, day 0 and 7) + running load (a day after first injection): treadmill 500 m/day with a speed of 500 m/h for 5 days/week until being sacrificed.	Kaiki, 1990 <sup>18</sup>	24	M	2. 5 m o n t h s o l d	350 g	2(n=3), 3(n=7), 5(n=7), 8 weeks(n =7)	-	Mankin score: the exact scores for each knee in each checkpoint has showed in the article: all scores were more than 6 at week 8	joint space narrowing (week 5) - joint structure destruction (week 5) - irregular cartilage surface (week 5) - reduced safranin o-fast staining (week 5)
Abbreviations: OARSI, Osteoarthritis Research Society International; KOA, Knee osteoarthritis; ACLT, Anterior cruciate ligament transection; pMM, partial Medial meniscectomy; MMP, Matrix metalloproteinase; MIA, Monoiodoacetate;											

**Supplementary Table 6. High fat diet models of knee osteoarthritis**

Intervention	Animal	Exact type of intervention	First author, year	Number of models	Sex	Age	Weight	Checkpoints after intervention	Osteophyte formation	KOA score	KOA related findings
regular diet	Wister rats	12 weeks of regular diet (9% of the kcal contained fat) + groove surgery at the end of 12 weeks of regular diet	De Visser, 2107 <sup>102</sup>	14	M	3 months old	.	12 weeks	-	-	synovitis - Lower mean thickness of trabecular bone and subchondral plate
	Lewis rats	8 weeks regular diet + DMM surgery 4 weeks after the start of diet	Ernest, 2018 <sup>103</sup>	40	F	2 months old	175 - 183 g before	8 weeks	8 weeks	-	Mild osteophyte formation
	C57BL/6 J mice	10 weeks low-fat diet (10% kcal from fat) + DMM surgery at the end of 10 weeks of low-fat diet + 8 weeks low-fat diet after the surgery	Warmink, 2020 <sup>104</sup>	10	M	3 months old	.	18 weeks	8 weeks	-	Osteophyte formation - cartilage degeneration - lower synovial lining thickness - fat pad fibrosis - lower subchondral thickness
High-fat diet only	Wister rats	12 weeks of High-fat diet (60% of the kcal contained fat)	De Visser, 2017 <sup>102</sup>	6	M	3 months old	.	12 weeks	8 weeks	-	osteophyte formation (lower than surgical + high fat diet group) - significant increase for total cholesterol and fasting insulin levels compared to the standard diet group
	C57BL/6 J mice	38 weeks of high-fat diet (45% kcal contained fat)	Warmink, 2020 <sup>104</sup>	10	M	3 months old	.	38 weeks	38 weeks	-	mild Fibrosis in the infrapatellar fat - Cartilage degradation (least) - mild Osteophyte formation - mild Adipose inflammation - mild synovitis
		4 weeks control-diet (13.5% kcal from fat) and then 12 weeks very high-fat diet (60% kcal from fat)	Griffin, 2012 <sup>106</sup>	5	M	2 months old	.	24 weeks	-	-	-
		4 weeks control-diet (13.5% kcal from fat) and then 12 weeks very high-fat diet (60% kcal from fat) + wheel running for 4 weeks parallel with final 4 weeks of very high-fat diet	Griffin, 2012 <sup>106</sup>	5	M	2 months old	.	24 weeks	-	-	Proteoglycan loss - significantly reduced subchondral bone thickness compared to high-fat diet + exercise group

		obesity and obligatory bipedal walking	Son, 2019 <sup>17</sup>	24	M	3 months old	31 ± 2.9 g	8,10,12 weeks	12 weeks	-	fibrillation (week 8) - proteoglycan loss (week 8) - Subchondral sclerosis (week 8) - cartilage loss (week 12) - synovitis (week 12) - osteophyte formation (week 12)
High-fat diet + surgery	Wister rats	12 weeks High-fat diet (60% of the kcal contained fat) + groove surgery at the end of 12 weeks of high-fat diet	De Visser, 2017 <sup>102</sup>	14	M	3 months old	.	12 weeks	12 weeks	-	osteophyte formation - degeneration of the articular cartilage - synovitis - increased joint inflammation - CD68 positive cells in synovium and osteophytes
	Lewis rats	8 weeks high-fat diet (60% of calories from fat, 20% from carbohydrates, 20% from protein) + DMM surgery 4 weeks after the start of diet	Ernest, 2018 <sup>103</sup>	10	F	2 months old	175 - 183 g before regime	8 weeks	-	-	-
		8 weeks High-fat diet (60% of calories from fat, 20% from carbohydrates, and 20% from protein) + sham surgery 4 weeks after the start of diet	Ernest, 2018 <sup>103</sup>	10	F	2 months old	175 - 183 g before regime	8 weeks	-	-	-
	C57BL/6 J mice	18 weeks high fat + DMM surgery 10 weeks after the start of diet	Warmink, 2020 <sup>104</sup>	10	M	3 months old	.	18 weeks	-	-	-
		10 weeks low-fat diet (10% kcal from fat) + DMM surgery at the end of 10 weeks of low-fat diet + 8 weeks high-fat diet after the surgery	Warmink, 2020 <sup>104</sup>	10	M	3 months old	.	18 weeks	18 weeks	-	moderate Fibrosis in the infrapatellar fat - moderate Cartilage degradation - moderate Osteophyte formation - moderate synovitis - moderate Adipose inflammation
	Wistar Han rats	24 weeks High-fat diet (20 kcal% protein, 40 kcal% fat of which 94% pork lard, 40 kcal% carbohydrates of which 83% sucrose) + groove surgery 12 weeks after the start of diet	Warmink, 2022 <sup>105</sup>	5	M	3 months old	.	24 weeks	24 weeks	-	Osteophyte formation - cartilage degeneration - fat pad fibrosis
Sprague Dawley rats	24 weeks High-fat diet (20 kcal% protein, 40 kcal% fat of which 94% pork lard, 40 kcal% carbohydrates of which 83% sucrose) + groove surgery 12 weeks after the start of diet	Warmink, 2022 <sup>105</sup>	5	M	3 months old	.	24 weeks	24 weeks	-	osteophyte formation (a much higher number of osteophytes compared to Wistar rat group) - osteoporosis-like decrease in trabecular bone volume - cartilage degeneration - fat pad fibrosis	
Abbreviations: OARS, Osteoarthritis Research Society International; KOA, Knee osteoarthritis; DMM, Destabilization of medial meniscus;											